An-Najah National University

Faculty of Graduate Studies

Photo-mineralization of aqueous gram positive and gram negative bacteria together with their organic components using sensitized ZnO nano-particles

By

Sawsan Fathi Abed- Al Salam Jaber

Supervisor

Prof. Hikmat Hilal

Co-Supervisor

Dr. Majdi Dwikat

This Thesis is Submitted in Partial Fulfillment of the Requirements for the Degree of Master of Chemistry, Faculty of Graduate Studies, An-Najah National University, Nablus, Palestine.

2018

Photo-mineralization of aqueous gram positive and gram negative bacteria together with their organic components using sensitized ZnO nano-particles

By

Sawsan Fathi Abed- Al salam Jaber

This Thesis was defended successfully on 24 /5/2018 and approved by:

Defense Committee Members	**Signature**
– **Prof. Hikmat Hilal / Supervisor**	.....
– **Dr. Majdi Dwikat / Co-Supervisor**	.....
– **Dr. Subhi Samhan/ External Examiner**	.....
– **Dr. Raed Alkowni / InternalExaminer**	.....

Dedication

My heart pulsates with the thrill for tendering gratitude to those persons who helped in completion for my project. To my husband, daughter, son, mother, sister and brother for their continuous support with my appreciation. The pleasant point of presenting a report is the opportunity to thank those who have contributed to build my knowledge. Unfortunately, the list of expressions of thank no matter how extensive is always incomplete and inadequate. Indeed, this page of acknowledgement shall never be able to touch the horizon of generosity of those who tendered their help to me.

Acknowledgment

I extend my deep sense of gratitude and indebtedness to my guide Prof. Hikmat Hilal for his kind attitude, keen interest, immense help, inspiration and encouragement which helped me carry out the work. I an extremely grateful to Dr. Majdi Dwikat and Dr. Ahed Zyoud for providing all kind of possible help throughout my project work. It is a great pleasure for me to acknowledge and express my gratitude to the whole teaching and non-teaching staff for their understanding, unstinted support and endless encouragement during my project.

Technical help, from Professor Naser Qamhieh, Department of Physics, UAVE University, Al-Ain, UAE, in measuring XRD and SEM, is acknowledged. Lastly, special thanks for Faculty of Agricultural Science and Technology in Palestine Technical University for their help in total organic content (TOC) analysis and for Palestinian Water Authority and Middle East Desalination Research Center (MEDRC)Fellowship for their support.

الإقرار

أنا الموقع أدناه مقدم الرسالة التي تحمل العنوان

Photo-mineralization of aqueous gram positive and gram negative bacteria together with their organic components using sensitized ZnO nano-particles

أقر بأن ما شملت عليه الرسالة هو نتاج جهدي الخاص, باستثناء ما تمت الإشارة إليه حيثما ورد، وأن هذه الرسالة ككل أو أي جزء منها لم يقدم من قبل لنيل أي درجة أو لقب علمي أو بحثي لدى أي مؤسسة علمية أو بحثية

Declaration

The work provided in this thesis, unless otherwise referenced, is the researcher's own work, and has not been submitted elsewhere for any other degrees or qualifications.

Student's Name: **اسم الطالب: سوسن فتحي عبد السلام جابر**

Signature **التوقيع:**

Date **التاريخ: 2018/5/24**

Table of Content

List of Abbreviations

Symbol	Abbreviation
a.u.	Arbitrary unit
ANU	An-Najah National University
AOP	Advanced Oxidation Processes
CB	Conduction Band
CFU	Colony Forming Unit
CPC	Compound Parabolic Collector
DBPs	Disinfection By-Products
DRS	Diffuse reflectance spectroscopy
e^-	Electron
E_g	Band gap
eV	Electron Volt
G	Gram
GrF	Graphite felt
h+	Hole
K .pneumoniae	*Klebsiella pneumoniae*
MG	Malachite Green
MIC	Minimal Inhibitory Concentration
MO	Methyl Orange
NPs	Nano- particles
PL	PhotoLuminescence Spectra
PT	Polythiophene
S. aureus	*Staphylococcus aureus*
SEM	Scanning Electron Microscopy
SG	Silica Gel
THMs	Trihalomethanes
TOC	Total Organic Carbon
UAE	United Arab Emirates University
UV	Ultraviolet light
VB	Valence Band
WHO	World health organization
XRD	X-Ray Diffraction

List of Tables

List of Figures

Photo-mineralization of aqueous gram positive and gram negative bacteria together with their organic components using sensitized ZnO nano-particles

By
Sawsan Fathi Abed- Al Salam Jaber
Supervisor
Prof. Hikmat Hilal
Co-Supervisor
Dr. Majdi Dwikat

Abstract

Photo-degradation is one of the most attractive methods. It involves excitation of the suitable semiconductor by light, followed by mineralization of biological and chemical pollutants in water. ZnO nanoparticles (ZnO NPs) are being used for photo-degradation of widely spread water organic pollutants. Due to its wide broad band gap (~3.2 eV), ZnO photo-catalytic activity is limited to shorter wavelengths which located in UV region. As only ~4% of the solar spectrum falls in the UV region, smaller band gap natural dyes, such as natural dyes(Anthocyanin) are examined to sensitize ZnO particles for visible solar light.

In this work disinfection of water by complete deactivation and mineralization of G +ve and G -ve bacteria, together with their organic components, using ZnO NPs was investigated. ZnO NPs are known as antibacterial agents, noxious to microorganisms, and hold good biocompatibility to human cells. Both naked ZnO and ZnO\Anthocyanin are tested against G –ve *K. Pneumonia*e and G +ve *S. aureus* bacteria by using direct solar light simulator.

The efficiency of ZnO-NPs revealed that using both synthesized and commercial ZnO-NPs, with and without Anthocyanin dye sensitizer under sun light simulator were used for deactivated bacteria, finding that after 60 min G +ve *S. aureus* and G –ve K. *pneumonia*e bacteria were totally deactivated. While after 3 hrs. 98.7% of G + ve *S. aureus* and 45.2% of G – ve *K. pneumonia*e bacteria organic matters were mineralized by using ZnO-NPs. These results confirm the ability of ZnO-NPs to behave as effective catalyst in photo mineralization of the two bacteria in water. It is therefore recommended to expand the present study and include other types of biological pollutants, in addition to study other factors that might impact photo mineralization reaction.

Chapter 1

Introduction

1.1 General.

Purified water is essential for living a healthy life. As such everyone should have access to it. Drinking water conditions have great impacts on people's everyday life, especially in the rural area where access to safe drinking water is extremely fateful. Climate change, population growth and increasing water scarcity, already create challenges for water supply systems. According to WHO, by 2025, half of the world's population will be living in water-stressed areas according to water demand [1]. As a result, Re-use of wastewater by water remediation is becoming an important strategy.

In recent days, more and more countries are using wastewater for irrigation. In developing countries this represents 7% of irrigated land [2]. If this practice is done in suitable way, safe management of wastewater can yield multiple benefits, including increased food production. Until this, options for water sources used for drinking-water and irrigation will continue to evolve, with an increasing dependence on groundwater and alternative sources, including wastewater. Reusing wastewater by purification it from all types of contaminants can be a real solution. Safe Drinking Water Act defines the term "contaminant" as any physical [3], chemical, biological, or radiological [4,5] substance or matter in water. Some drinking water contaminants may be harmful if consumed at certain levels in drinking water

while others may be harmless. The presence of contaminants does not necessarily indicate that the water poses a health risk.

1.1.1. Biological contaminants.

Naturally, Water contains a various population of living organisms, such as aquatic plants, bacteria, parasites and viruses. Some of them are harmless while others can be harmful to humans. Every year 1.5 million people die as a result of diarrhea and other diseases caused by unclean water and poor sanitation [6]. The WHO Guidelines for Drinking Water Quality recommend that all water intended for drinking should have zero *fecal coliform* contamination in 100 ml sample.

1.1.2. Bacteria.

Bacteria are the most common microorganisms found in animal and human feces. Drinking water contaminated by feces is the primary cause of water-borne infections, with some bacteria. Only a few cell found in water can be pathogenic [7].

1.1.2.a. G +ve and G –ve bacteria.

G staining is a common technique used to differentiate between two large groups of bacteria based on different cell wall contents. Table (1.1) shows common differences between G +ve and G –ve bacteria.

Table (1.1): The most common differences between G +ve and G –ve bacteria [8-10].

	Gram negative bacteria	**Gram positive bacteria**
Gram reaction	Can be decolourized to accept counter stain (Safranin or Fuchsine); stain red or pink, they don't retain the G stain when washed with absolute alcohol and acetone.	Retain crystal violet dye and stain dark violet or purple, they remain colored blue or purple with G stain when washed with absolute alcohol and water.
Peptidoglycan layer	Thin (single-layered).	Thick (multilayered).
Outer membrane	Present.	Absent.
Resistance to physical disruption	Low.	High.
Cell wall composition	The cell wall is 70-120 Å, thick; two layered. Lipid content is 20-30% (high), Murein content is 10-20% (low).	The cell wall is 100-120 Å thick; single layered. Lipid content of the cell wall is low, whereas Murein content is 70-80% (higher).

1.1.3. *Klebsiella pneumoniae.*

A Gram -ve bacterium with large polysaccharide capsule that distinguishes the organism [11].

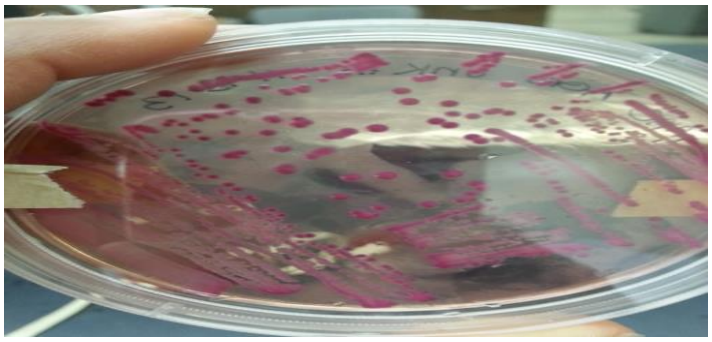

Figure (1.1): A pink G –ve stain *K. pneumonia* of cells.

1.1.3.a. Human health effects.

K. pneumonia have been identified as colonizing hospital patients, where spread is associated with the frequent handling of patients (e.g. in intensive-care units). Patients at highest risk are those with impaired immune systems [12]. Patients with *K. pneumonia* infection have an increased tendency to develop lung abscess, cavitation, empyema, and pleural adhesions [13-15].

1.1.4. Staphylococcus aureus.

A G -ve with non-moving small round shaped. They are approximately 0.5-1.5 µm in diameter [16].

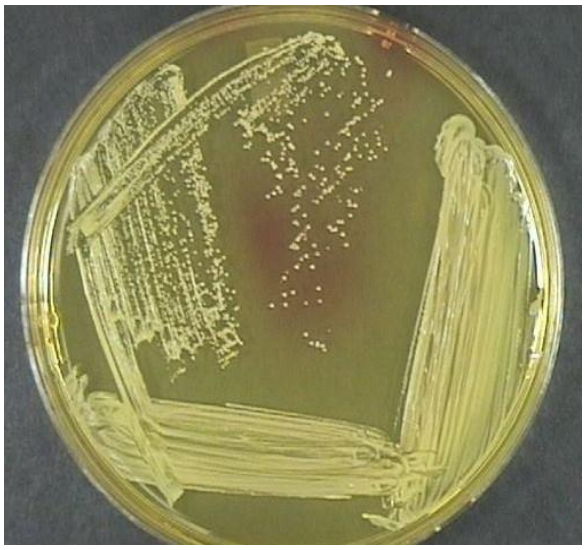

Figure (1.2): G +ve stain of *S. aureus*cells.

1.1.4.a. Human health effects.

Although *S. aureus* is a common member of the human microflora, it can produce disease. Based on the ability of the organisms to multiply and spread widely in tissues [17].

1.1.4.b. Source and occurrence.

S. aureus is relatively widespread in the environment but is found mainly on the skin and mucous membranes of animals. *S. aureus* is occasionally detected in the gastrointestinal tract and can be detected in sewage. *S. aureus* can be released by human contact into water environments such as swimming pools, spa pools and other recreational waters. It has also been detected in domestic water [18,19].

1.1.5. Water purification.

Advanced Oxidation Processes (AOPs) using hydroxyl radicals and other oxidative radical species are being studied extensively for removal of various pollutants from wastewater. Many AOPs ozonation, chlorination, UV/ozone, UV/hydrogen peroxide, and UV/photocatalysis are most commonly studied and used in many applications [20].

Unfortunately, the common disadvantage shared between all sorts of AOPs is the high operating cost, which has somewhat limits large-scale applications. Moreover, the side effect of some AOPs could effect on the human health. For example, in the 1970s scientists discovered that when chlorine is added to water, it forms Trihalomethanes (THMs), one of which is chloroform. THMs increase the production of free radicals in the body and are highly carcinogenic (cancer causing) [21].

On the other hand, research started focusing on using heterogeneous-semiconductor photo-catalysis for water disinfection. The effectiveness of these semiconductors against microorganisms including bacteria, viruses, protozoa and fungi have been proved as illustrated in (Chapter 2). It is generally reported that the photocatalytic disinfection of water requires exposure to irradiation of equivalent or higher energy than the band gap of the semiconductor. The distance between the valence and conductivity bands amounts to 0.7-3.5 eV for semiconductors and is called a Band gap, Eg. Table:(1.2) shows values of band gaps of some common semiconductors. Zinc Oxide is classified as a semiconductor in group II-

VI, whose covalence is on the boundary between ionic and covalent semiconductors. A broad energy band (3.2-3.37 eV) with high thermal and mechanical stability at room temperature make it attractive for potential uses [23]. Zinc Oxide, has unique physical and chemical properties, such as high chemical stability, high electrochemical coupling coefficient, broad range of radiation absorption and high photo-stability

Table (1.2): Band gap widths of some more popular semiconductors [22].

Semiconductor	Eg (eV)
Si	1.1
Fe_2O_3	2.3
CdS	2.5
TiO_2 (rutile)	3.0
TiO_2 (anatase)	3.2
ZnO	3.2-3.37
SnO_2	3.5

In addition, ZnO was extensively studied as antimicrobial agent due to its photocatalytic activity under UV light. Its nano-powders are generally used as effective and nontoxic semiconductor photo-catalyst for the degradation of different organic chemicals and synthetic dyes. The studies showed that ZnO NPs were more abrasive than bulk ZnO. The nano size of ZnO contributes to the greater mechanical damage to the cell membrane and the enhanced bactericidal effect [24].

1.1.6. Zinc Oxide Sensitization.

Stable oxide semiconductor types could not absorb visible light because they have wide band gaps. For ZnO is a wide band gap semiconductor with wide

band gap (3.2 -3.37 eV) at room temperature [25]. To solve this problem, the wide band gap semiconductor materials was sensitized. Sensitization of ZnO with dyes, such as organic dyes, can enhance the potential of light absorption by exciting and injecting electrons into Conduction Band(CB) of the semiconductor. Here, in this work, "low cost, abundant, easily extractable and safe material" are the set conditions for the dye to use. Anthocyanin dye satisfies these conditions. Thus, it has been used as a photosensitizer for Zinc Oxide sensitization. The dye is extracted from local plants.

1.1.7. Anthocyanin Dye.

Natural dyes are abundant, easily extractable, safe and cause no environmental threat. Besides betalains, carotenoids and chlorophyll, Anthocyanins, the most important group of natural dyes widespread in nature. Most often they are present in leaves, fruits and flowers [26]. Anthocyanins are plant polyphenols. They involve derivatives of 2-phenylbenzo pyrylium salts (flavylium salts). The aglycone moiety is glycosylated by one or more sugars and can have several hydroxyl and methoxy groups. It contains delocalized electrons and is responsible for the color of the compound. Anthocyanins absorb light in a range of 520-550 nm [27]. Fig. (1.3) shows some possible structural formulas for different Anthocyanin structures.

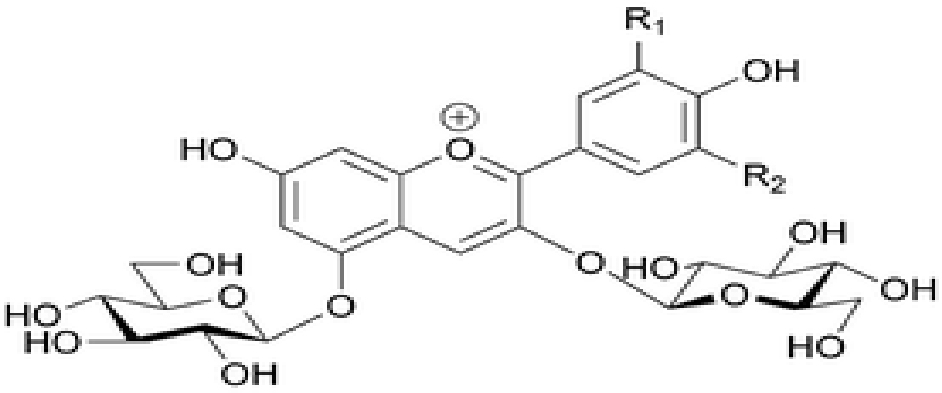

R_1	R_2	anthocyanin	aglycon
H	H	pelargonin	pelargonidin
OH	H	cyanin	cyanidin
OCH_3	H	peonin	peonidin
OH	OH	delphin	delphinidin
OCH_3	OH	petunin	petunidin
OCH_3	OCH_3	malvin	malvidin

Figure (1.3): Structures of common Anthocyanins and their Aglycons [28].

Due to this, Anthocyanin dye was chosen here for Zinc Oxide sensitization. It is extracted from flowers petals of Hibiscus tea (*karkade*) available in local market.

1.1.8. Proposed mechanism for naked nano-ZnO effect:

Zinc Oxide has a energy band gap of ~3.37 eV [9]. When the energy of a photon from the light source exceeds this gap, $\lambda \approx 368$ nm, a photo-excited electron will be promoted to the conduction band (CB) leaving a positive hole in the valence band (VB).

$$ZnO + h\nu \rightarrow e^-_{CB} + h^+_{VB} \qquad (6.1)$$

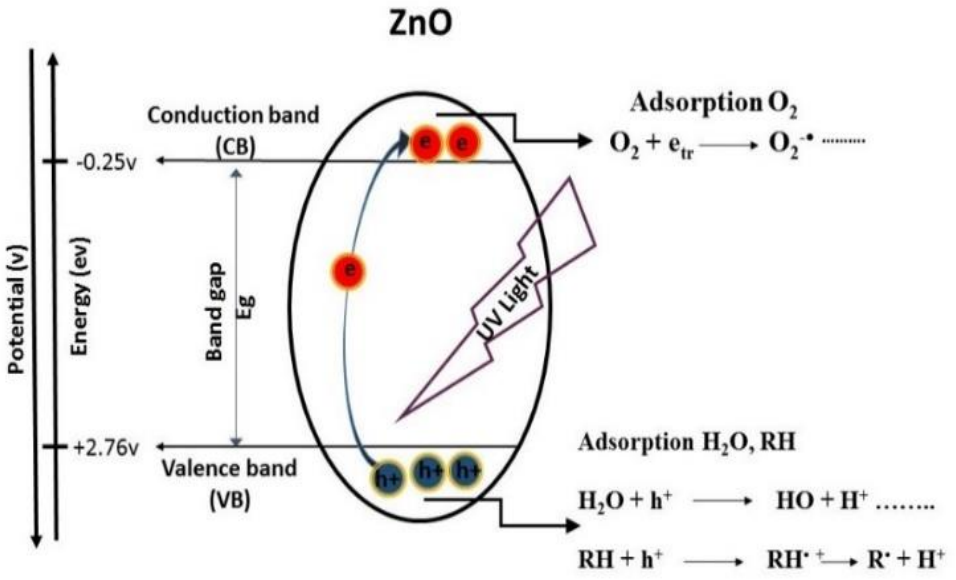

Figure (1.4): The mechanism of naked semiconductor photocatalysis.

If the photo-holes and photo-electrons produced by this process migrate to the surface, then interact with adsorbed species. The positive hole will react with adsorbed water molecules on the surface of semiconductor producing ($OH^{\bullet}$) radicals and the electron will react with adsorbed oxygen on the surface producing superoxide ions ($O_2^{\bullet-}$). Generally, hydroxyl radical ($OH^{\bullet}$) and superoxide ions ($O_2^{\bullet-}$) are primary free radicals since both of them can be generated by metal oxide directly. Other radicals such as singlet oxygen($^1O_2$), hydrogen peroxide (H_2O_2) can be formed indirectly by a series of photochemical reactions involving either hydroxyl radical ($OH^{\bullet}$) or superoxide ions ($O_2^{-\bullet}$).

The procedure can be summarized as described by literature for organic contaminants [56-57].

These free radicals are very unstable and reactive with other compounds, trying to capture the needed electron to gain stability. Stimulation of oxygen

species such as H_2O_2, O^{-2} and $OH^{\bullet}$ by UV light harms bacteria and damages the active enzyme, DNA, and protein [58-59]. The species oxidize the cell membrane of bacteria, and the compounds. When the "attacked" molecules lose their electrons, they become free radicals themselves and a chain reaction begins [61]. Free radicals will not attack cell membrane only, but as we propose it will degrade all cellular components (mainly DNA, RNA and lipids) coming out from deactivated bacteria. In dark deactivation of bacteria occurs due to ZnO NPs toxicity which disturbs the cell's metabolic system of bacteria and deactivates them [29-37, 60].

1.2 Objectives.

The major objective of this work is "Disinfection of water by complete deactivation and mineralization of G+ ve and G –ve bacteria by using a low cost and safe method of photo mineralization".

Chapter 2

Literature Review

– In 2012, B. Subash and his team synthesized Zr co-doped Ag-ZnO and used it for the degradation of red 120 dye under natural sun light illumination, first they tested several metallic doped with Ag-ZnO finding that 4% wt Zr co-doped Ag- ZnO Almost achieved complete degradation of the dye takes place at the time of 30 min under solar light. 50.0% decrease in dye concentration occurred in the absence of solar light. However, using Ag metal will increase the cost of this catalyst and in general it's not favorite to add many types of metals to water here, such as Ag and Zr in addition to Zn, this will effect on both the taste of drink water and heath [29].

– In 2014 different composites of Polythiophene (PT)/Zinc Oxide (ZnO) nanoparticles with different PT weights were synthesized by M. Khatamian and his team. Chemical oxidative polymerization was used for the preparation of composites, with average particle size of 30 nm of ZnO. Optical properties of the prepared composites were investigated by Diffuse Reflectance Spectroscopy (DRS) which showed a broad peak in the visible region which its intensity increased by increasing the PT percentage. The photocatalytic activities of the composites were evaluated by degradation of Methyl Orange (MO) aqueous solution under visible light (9W LED lamp; whitelight,400–700nm), sunlight irradiation and dark. The composition of ZnO with

PT in the composites improves its adsorption capacity in the dark, higher removal percentage is obtained at 30 min, using PT (20%)/ ZnO samples the adsorption capacity reach to 75%. While under visible light the removal efficiency of pure ZnO is 48% in 180min irradiation time. Moreover, TOC result for the PT (20%)/ZnO composite is lower than pure ZnO after 180 min [30].

– In 2015, different morphologies of ZnO nanomaterials were synthesized and used as photo-catalyst for self-sensitized photo-degradation of Malachite Green (MG) under solar light. Finding that ZnO flowers exhibited highest photocatalytic activity, with complete mineralization of dye to produce CO_2 [31].

– In 2016, Venieri and his team worked on doping titania with non-metals which decrease its band gap energy below the value of 3.2 eV, then the disinfection potential of cation-doped titania in terms of *S. aureus* elimination in aqueous samples under artificial and natural sunlight was investigated. Fe, Al and Cr doped TiO_2, the relative activity for *S. aureus* inactivation decreased in the order Fe-TiO_2> Al-TiO_2> Cr-TiO_2. This could achieve a 99.9% deactivation of *S. aureus* population after 60 min. On the other hand, they mentioned how $Cr^{3+}$is generally harmless in the environment due to its weak membrane permeability. And also toxicity of $Al^{3+}$is highly dependent on the pH of water and organic matter content. With decreasing pH its toxicity increases, so these metals may alone cause *S. aureus* inactivation and be another sources of pollutants in water. In addition,

they did not talk about the stability of catalyst and proposed that it worked in principle of forming free radicals which causes damaged in the bacterial cell membrane, however, forming these radicals meaning also forming holes with positive charge and cation-doped titania may resist dispose of these holes [32].

– In 2016, Synthesis of ZnO/ZnS core/shell nanoparticles by grown a shell of ZnS over synthesized ZnO nanoparticles. Absorption spectroscopy of core/shell was done finding blue shift in the UV visible absorption spectra. Then photo-catalysis tests were done by degradation methylene blue in water. Knowing that both Zinc Sulphide (ZnS) and ZnO having band gaps 3.72 eV and 3.37 eV, but they proposed that the band gap of the core–shell system is smaller than both the core and the shell material and this proved by dye degradation. However, in some cases electron–hole recombination occurs at the interface between the core and the shell material and this can reduce the photocatalytic activity [33].

– In 2017, a novel combined solar system consisting of a TiO_2 thin-film annular photoreactor and a pasteurizer operating under continuous flow designed was tested, to improve both the bacteria inactivation and organics degradation. With reducing cost because works without pumps or a power supply. The simultaneous *E. coli* inactivation and degradation of the pharmaceutical antipyrine in synthetic urban wastewater using this system was studied. as a function of hydroxyl radical generation by solar TiO_2 activation. The chemical degradation

and bacteria photo-inactivation kinetic modelling and rate-limiting step in the TiO_2 compound parabolic collector (CPC) were evaluated. 99.1% of bacteria photo-inactivation was reached in the TiO_2/CPC system (0.60 mg cm^{-2}) with time 80 min. Chemical decontamination increased with increasing residence time and increasing TiO_2 load in the CPC. Up to 70% antipyrine removal was achieved under the studied operating conditions. The addition of 150 mg L^{-1} of H_2O_2 in the CPC at the beginning of the reaction improved the process efficiency by generating extra radicals. Both the antipyrine degradation and *E. coli* photo-inactivation were found to be catalyst surface reaction-rate controlled in the solar/ H_2O_2/TiO_2 photoreactor [34].

– In 2017, ZnO/SG by the molten salt $ZnCl_2$ method was successfully prepared. In their technique, no reduction agent was used. Hence, it is an environmentally friendly method. Furthermore, the entire process lasts about 2 hours. After 60 min, the cluster of nanoparticles was seen, and around 90 min, plenty of ZnO nanoparticles covered the SG. The antibacterial test of the samples against *E. coli* and *S. aureus* shows all bacteria were deactivated after 40 min. The antibacterial results detected that the ZnO/SG prepared in longer deposition times possess better antibacterial activity due to the improvement in the contents of ZnO nanoparticles on the silica surface. However, in their research they did not deeply look how bacteria is deactivated and if

their catalyst could work with another types of pollutants such as chemical pollutants [35].

– In 2017, electrochemical oxidative degradation of diazo dye amido black 10B (AB10B) as model pollutant in water has been studied by using nanostructured ZnO-TiO_2 thin films deposited on graphite felt (GrF) substrate as anode. The best operating conditions for the degradation of 0.12 mM (74 mg L^{-1}) dye concentration and mineralization of its aqueous solution were determined as GrF-ZnO-TiO_2 thin film anode, 100 mA current intensity, and 0.1 mM Fe^{2+} (catalyst) concentration. Under these operating conditions, discoloration of AB10B solution was reached at 60 min while 6 h treatment needed for a mineralization degree of 91 %. Finally, they proposed that treatment with GrF-ZnO-TiO_2 composite thin film anode that seems to be the most powerful electrode for an efficient removal of AB10B dye from water. However, using electrochemical oxidative process for water purification increasing the cost [36].

– In 2017, a team from Hanyang and Shivaji Universities investigated the effect of structure, morphology and chemical doping of metal oxide (ZnO) on its photocatalytic activity and experiment it towards the degradation of methyl orange. At low temperature a facile and template free reflux method has been used to synthesize ZnO nanostructures for the morphology control of cubes, maize corn seeds and rods, finding the ZnO maize corn seed shaped shows the superior photocatalytic activity which offering smaller crystallite size and

more intensity of polar plane (002) that may provide more active sites for photocatalytic reactions. Then enhanced the photocatalytic activity by 0.5 mol% Cu ions substituting in maize corn seeds. However, the band gap of ZnO nanostructures increased from 3.38 to 3.46 eV because of Cu provides free carriers which shift the Fermi level meaning degradation process will occur under UV light illumination [37].

– In 2017, Multi ferrocenylimines compounds were synthesized and investigated their antibacterial properties against twelve different bacterial strains, finding that the most active ferrocenylimines compound was compound 3 which is N-(3-bromo-5- chlorosalicyl)-4-ferrocenylimine with a Minimal Inhibitory Concentration (MIC) value of 0.30 mg/ml against *S. sonnei*. On the other hand, further studies are essentially to investigate the toxicology of ferrocenylimine compounds [38].

2.1 Novelty of this work:

Bacterial infectious diseases are a serious health problem that has drawn the public attention worldwide as a human health threat, which extends to economic and social complications.

This research will investigate how naked ZnO and ZnO/ Anthocyanin catalysts can deactivate both G -ve *K. pneumonia*e and G +ve *S. aureus* bacteria under simulated sun light for the first time. As G +ve *S. aureus* bacteria have thicker cell walls, but G -ve *K. pneumonia* bacteria are more

resistant due their capsule nature, both types of bacteria will be investigated here comparatively for the first time. The ability of both bacteria to be deactivated and completely mineralized by different ZnO photo-catalyst systems, under different conditions will be assessed here.

ZnO NPs have been used by researchers as antibacterial materials. Two researches at ANU worked on ZnO NPs. Ateeq [48] investigated Anthocyanin sensitized ZnO catalyst in water disinfection from G -ve *(E Coli)* bacteria, while Ishtaiwa [49] used ZnO NPs in photo- degradation of G –ve (*E Coli* and *P. aeruginosa*) bacteria exposed to solar sun light containing UV radiation. TOC analysis was studied. Un like earlier literature [29-38]. An-Najah group have deactivated the G -ve bacteria and totally mineralized their organic content into mineral species.

Chapter 3

Materials and Methods

3.1 Materials.

3.1.1. Zinc Oxide.

Two types of ZnO particles were used, commercial powder (catalog no. 205532) was taken from (Sigma Co.) and directly used for photo-degradation of water samples or treated for sensitization. Synthetic ZnO was prepared from zinc acetate from (Sigma Co.) and sodium hydroxide from (Frutarom Co.). Both ZnO powders were used to prepared ZnO/Anthocyanin systems.

3.1.2. Anthocyanin Dye.

Anthocyanin dye was extracted from the flower petals of Hibiscus tea (karkade) in ethanol and supported onto ZnO particles to form the dye-sensitized photo-catalyst. Karkade was purchased from local markets.

3.1.3. Bacteria.

Both G +ve *S. aureus* and G –ve *K. pneumoniae* bacteria were chosen as examples of species for test disinfection mechanism of Zinc Oxide. These bacteria were isolated from clinical specimens and obtained from Medical Laboratory Sciences Department at ANU.

3.1.4. Other Chemicals.

Ethanol, sodium hydroxide and hydrochloric acid were all purchased from either Aldrich-Sigma Co. or Frutarom Co. as analytical grade, and were used as received without further purifications. Nutrient broth was purchased from Hi Media Laboratories Pvt. Ltd, India and nutrient agar was bought from Becton, Dickinson and company Sparks, USA, which were used for bacteria culturing and treatment.

3.2 Instruments.

3.2.1. UV–Visible spectrophotometry.

A Labo Med, Inc. 1601spectrophotometer was used to measure bacterial concentration. Quantitative determination of bacterial concentration was performed using turbidometric methods. By measuring the amount of light that passed through a suspension of cells. More cells have more turbidity and more turbidity means less light passing through the suspension. Working at 630nm wavelength and at absorptivity range (0.08-0.1) means having initial bacterial concentration equal 1.5 * 10^8CFU\mL and this according to 0.5 McFarland standard turbidity [39].

Solid state UV-Visible electron absorption spectra were measured for ZnO and ZnO/Anthocyanin systems and Anthocyanin dye concentration before and after sensitization. Measuring concentrations of Anthocyanin dye was performed at 550 nm wavelength.

A shimadzu UV-1601 spectrophotometer, equipped with a thermal printer Model DPU-411-040, type 20BE, was used. For solid ZnO particles, the spectra were scanned on 0.1 g of catalyst was suspended in 50 ml distilled water.

3.2.2. PhotoLuminescence Spectra (PL)

Prepared ZnO systems were characterized using fluorescence spectra. A Perkin-Elmer LS50 Luminescence Spectrophotometer was used to measure the emission fluorescence spectra. Catalyst (0.1 g) was suspended in 50 ml distilled water. The samples were excited by a suitable wavelength (350 nm). Emission spectra were used to calculate semiconductor catalyst band gaps which were compared with literatures values [22-25]. The spectra were studied for naked and sensitized ZnO systems (prepared nanoparticles and commercial ones).

3.2.3. Sun Light Simulator.

A MEDIUM 536p lamp was used as sun irradiation simulator with Lamp 36V\ max 400 W to fix amount of light intensity on samples at constant time. Moreover, the wave length passing through polluted water was controlled, so as get more accurate results.

3.2.4. Lux-meter.

A Lux-meter (Lx-102 light meter) was used to measure the intensity of radiation at the tested polluted water to determinate the efficiency of both

naked and sensitized catalyst. The recorded value was ~ 100000 lux (similar to solar light intensity).

3.2.5. XRD.

X-ray diffraction was used to determine crystallinity of the catalyst. It is primarily used for distinguishing between amorphous and crystalline material and quantification of the percent crystallinity of a sample. The XRD patterns of the powdered samples were recorded using Philips XRD XPERT PRO diffractometer with CuK with X-ray wavelength (λ = 1.45 Å). The analysis was kindly performed at UAE University, Al Ain, UAE.

3.2.6. SEM.

SEM images of the samples were taken using a Jeol Model JSM-6700F. The analysis was kindly performed at UAE University, Al Ain, UAE.

3.2.7. TOC.

The Total Organic Carbon (TOC) as equivalent of water organic content was used to evaluate the mineralization degree of treated aqueous solution. The decrease of solution TOC means the conversion of organic matter present in the solution to CO_2mainly by free radicals generated in the process. Inorganic carbon was determined by acidification the sample by 1 % hydrochloric acid before injection and organic carbon was measured by burning the sample ~at 800 ^{o}C. The Total Organic Carbon (TOC) was measured using a SHIMADZU Model TOC-L CSH\CSN. Each

measurement was repeated three times, and the result is calculated from the average of the two closest values. The analysis was kindly performed by Faculty of Agricultural Science and Technology at Palestine Technical University.

3.2.8. pH Meter.

Controlling pH values for experiments and extracted dye to determine the amount of dye stuck on the surface of the catalyst, this by measuring the concentration of dye before and after sensitization process.

3.2.9. Thermometer.

A simple mercury thermometer was used to measure temperature during preparation and deactivation processes.

3.2.10. Other devices.

Centrifuge scientific Ltd model 1020 D.E, Vortex, Incubator, Micropipette, Autoclave and Glasses.

3.3 Preparations.

3.3.1. Preparation of ZnO NPs.

Synthesis ZnO NPs by precipitation method was achieved as follows: Aqueous solution (0.45 M) of zinc acetate ($Zn(CH_3CO_2)_2$) was prepared by dissolving 15.231 g in 150 mL distilled water. The solution was then diluted to 250 mL in a volumetric flask. An aqueous solution of 0.9 M sodium hydroxide (NaOH) was prepared by dissolving 9.0 g NaOH in 200 mL

distilled water, and the solution was then diluted to 250 mL in a volumetric flask. The NaOH solution was then poured into a 500 mL beaker and heated to 55-60 °C. The $Zn(CH_3CO_2)_2$ solution was added drop wise over a period of 40 minute, to the heated NaOH solution under medium speed magnetic stirring. The beaker was covered by glass dish for 24 hours to make sure that white fine ZnO NPs precipitated. Then water was removed by decantation. The precipitate was washed several time with deionized water and ethanol to remove all ions which might be stuck on its surface and then dried under air at about 60 °C over night [84].

3.3.2. Anthocyanin Dye Extraction.

Dried *(karkade*) plants flowers (40 g) were crushed into small pieces and drenched with 100 ml ethanol and few drops of concentrated HCl with continuous magnetic stirring for 1 hour. The extracted dye was then filtered, and acidified at pH < 1 to make it stable [64]. The extracted dye (later used to sensitize both synthesized and commercial ZnO powders) was then stored in a dark-color glass flask for further use.

3.3.3. Zinc Oxide/Anthocyanin Dye Preparation.

ZnO NPs (10 g) were mixed with 100 mL of 76×10^{-5} mol\L extracted amount of Anthocyanin dye, then stirred magnetically for 30 min. in a 250 ml volumetric flask at room temperature. The mixture was then covered and left in the dark overnight to precipitate the resulting solid. The solid was then centrifuged and dried in air away from light for further applications. Both commercial and synthesized ZnO were treated with Anthocyanin as described above [48].

3.3.4. Preparations related to bacterial treatment.

Both G +ve *S. aureus* and G -ve *K. pneumoniae* were obtained from Medical Laboratory Sciences Department in ANU. Cultures of both types were prepared similarly. Nutrient agar was used as growth medium for measuring the remaining bacteria after the photo-degradation process. Nutrient agar was prepared according to manufacturer instructions and poured in Petri dishes after being autoclaved. Nutrient broth was used for micro-organisms inoculums preparation. It was also prepared according to manufacturer instructions and 5 ml of nutrient broth were poured in several test tubes. Normal Saline solution (0.9 %) was prepared by dissolving 9.00 g of NaCl salt in 1000 mL distilled water. 9 ml samples were taken and placed in each test tube. The saline solution was used to prepare fold dilutions of bacteria in polluted water samples to count bacteria. All prepared nutrient agars, nutrient broth tubes and normal saline tubes were autoclaved at 121^{o}C under 1.5 atm, and saved in cold condition(~4^{o}C) for further analysis. For bacterial preparations, a few colonies were put in 5 ml nutrient broth tube and incubated for 2-4 hours at 37^{o} C. Then the sample was analyzed by using UV–Visible spectrophotometry at 630 nm wavelength. Growing bacteria were diluted until device reading was in the range (0.08 - 0.10). Thus, McFarland concentration was obtained and the concentration of bacteria is assumed to be 1.5 x 10^{8} CFU/mL [39]. In all experiments 1x 10^{6} CFU/mL bacterial concentration was treated. This concentration was obtained by the following equations:

$$(Molarity_1 \times Vol._1)\ conc. = (Molarity_2 \times Vol._2)\ dil. \quad (1)$$

$$(1.5 \times 10^8\ CFU/mL_1 \times Vol._1)\ conc. = (1 \times 10^6{}_2 \times 50mL_2)\ dil. \quad (2)$$

$$Vol.1\ taken\ from\ concentrated\ bacterial\ solution = 0.330\ mL.$$

* Where, Moarity$_1$ is McFarland concentration which obtained by UV–Visible spectrophotometry at 630nm wavelength (1.5 x 10^8 CFU/mL).

* Vol.$_1$ is taken from McFarland concentration.

* Molarity$_2$ is needed bacterial concentration to be treated in 50 mL sample.

* Vol.$_2$ is sample volume (50 mL) [48-49]

3.4 Methods.

3.4.1. Experimental steps for disinfection of bacteria.

As in Fig. (3.1) each beaker contained 50 mL autoclaved distilled water. The first was called control sample which contained only bacteria. The second beaker contained bacteria treated with naked ZnO or ZnO/Anthocyanin. Two beakers were treated under sun simulated light and two beakers were treated in dark.

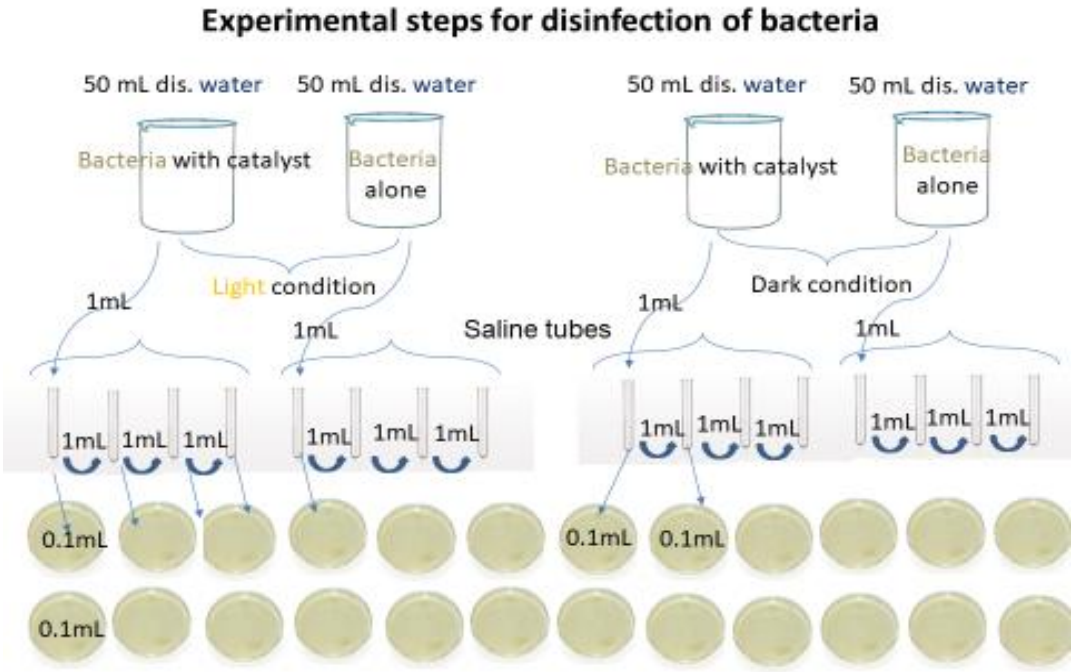

Figure (3.1): Experimental steps for bacterial deactivation by using several catalyst systems**.**

Finally, for all experiments and at the end of selected time, 1000 µL of each treated sample was withdrawn using a micropipette and diluted in a series of saline solution tubes with different dilutions (0.1, 0.01, 0.001 dilutions). From each diluted, aliquots of 0.1 mL were taken by yellow tip and were spread on two nutrient agar Petri dishes using bent glass rod, then incubated for 24 hrs at 37 °C. After incubation, the bacteria were grown and colonies in each plate were counted using plate count method, only plates which have colonies between 30 and 300 colonies were considered. The average number of each two plates for each dilution was calculated and the bacteria concentration as CFU/mL unit was reported according to the following equation:

$$\text{Bacterial conc.} = \text{Average number of colonies} \times \text{Dilution factor} \times 10 \quad (3)$$

$$The\ deactivation\ percent = \left(Conc._{initial} - Conc._{final}\right) \div Conc._{intial} \times 100\% \quad (4)$$

– Where, $conc._{initial}$ is bacterial initial concentration.

– $conc._{final}$ is bacterial final concentration.

The initial concentration was taken from the control samples, and the final concentration was taken from treated samples with ZnO types. These experiments were tested for both G +ve *S. aureus* and G –ve *K. pneumonia*.

Cutting-off experiment was done by using light cut-off filter which eliminated ~4% of UV-light found in sunlight simulator. The 400 nm and shorter wave lengths were removed. This was done on three samples: the first contained bacteria only, the second was naked 0.1 g ZnO with bacteria and the third was 0.1 g ZnO\Anthocyanin with bacteria. This experiment was made to distinguish between both naked and sensitized ZnO efficiencies against bacteria under visible light with no UV [48,49].

3.4.2. Impact of different parameters on bacteria mineralization.

The impact of different parameters on photo-mineralization efficiency were studied as the following: -

3.4.2.1. Impact of time.

At the beginning, several periods for bacterial deactivation were tested. Then 15 min and 60 min were chosen. After 15 min the differences between two ZnO systems were observed. After 60 min total bacterial deactivation was achieved. As a result, different reaction times (15, 60 min) were tested with constant 0.1g catalyst amount and 1×10^6 CFU\mL bacterial concentration at temperature 30ºC and pH~ 7. This was done for ZnO and ZnO\Anthocyanin against *S. aureus* and *K. pneumoniae* respectively under irradiation using sun light simulator.

3.4.2.2. Impact of catalyst amount.

low catalyst loadings, for economic purpose were used. (0.0,0.025, 0.05, 0.10) Gs were varied for samples with using two types of catalysts, naked and sensitized ZnO at different times (15, 60) min with constants bacteria concentration 1×10^6 CFU\mL, at 30ºC and pH~ 7 under irradiation using sun light simulator.

3.4.2.3. Impact of bacterial concentration.

Different concentrations of bacteria (1×10^6, 0.50×10^7, 1×10^7, 0.50×10^8 CFU\mL) were studied. This was to study the impact of increasing bacterial concentration on the mineralization efficiency.

3.4.2.4. Impact of stirrer type.

Three different stirring types were used. The first was without moving the sample, the second sample was stirred with shaking and the third was magnetically stirred. Thus, the influence of movement on deactivation process was studied.

3.4.2.5. Impact of pH and Temperature on catalyst efficiency.

By taking Ateeq and Ishtaiwa work into consideration and some literature review related to the bacteria growth conditions, pH and Temperature were used [48,49,51,52].

3.4.2.6. Catalyst recovery and reuse.

After the first photo-mineralization process was complete, the treated solution was autoclaved and the catalyst was decanted from water. It was then washed with water several times, and reused for second time.

Chapter 4

Results and Discussion

4.1 Introductory Remarks.

Main goal for this research was to disinfect water by complete deactivation and mineralization of a G +ve (*S. aureus*) and G –ve (*K. pneumonia*e) bacteria by using low cost, safe method accomplished with solar light. Naked ZnO and ZnO modified with natural Anthocyanin dye were prepared. Both systems were characterized using PL, Electronic Absorption Spectrum, SEM and XRD instruments. ZnO systems were then used to catalyze the photo-mineralization against G +ve (*S. aureus*) and G –ve (*K. pneumonia*e) using simulated light. A cut-off filter experiment was done to check if Anthocyanin dye impacts ZnO work in polluted water. Complete mineralization of bacteria and their organic contents was tested by measuring TOC in reaction mixture. Finally, factors impacting photo-mineralization reaction and catalyst efficiency, such as illumination time, temperature, pH, catalyst concentration, polluted concentrations were investigated.

4.2 Catalyst Characterization.

4.2.1. PhotoLuminescence Spectra (PL).

The photoluminescence (PL) emission spectra were measured for prepared and commercial ZnO and ZnO\Anthocyanin NPs. The purpose is to find E_g for each ZnO system and to find if sensitization process shifts E_g to left (visible region). As shown in Fig. (4.1) PL spectra collectedat350 nm excitation wavelength and maximum wave lengths (nm) were remarking in spectra for each system.

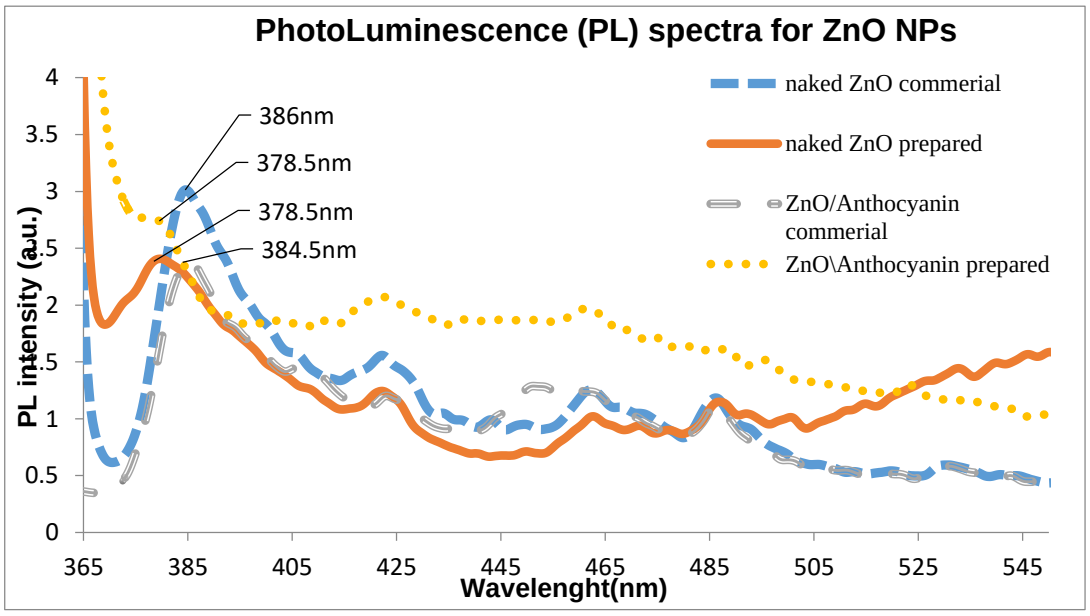

Figure (4.1): PhotoLuminescence (PL) spectra of 0.1 g ZnO NPs dispersed in 50 mL distilled water under 350 nm UV excitation wavelength, for prepared and commercial, naked and sensitized ZnO NPs.

By using equation ($Eg\,(eV) = hc \div \lambda max\,(nm)$) and intense emission peaks shown in Fig.(4.1), the E_g values for ZnO systems were calculated, as summarized in Table (4.1).

Table: (4.1) Wavelengths(nm) found on highest point in PL spectra and energy Band Gap determined by E_g equation, for ZnO systems.

	Naked commercial ZnO	Naked prepared ZnO	Commercial ZnO\Anthocyanin	Prepared ZnO\Anthocyanin
λ(nm)	386	378.5	384.5	378.5
E_g(eV)	3.21	3.28	3.22	3.28

As in Table (4.1) both naked ZnO systems give (3.21, 3.28 eV) Band Gap values. Our results are within the literature range of ZnO (3.2-3.37 eV) [22-25]. However, sensitization ZnO with Anthocyanin dye does not lower E_g to the visible region as expected and this is clear in Table (4.1). E_g gives indication about particle size [82]. When E_g value increase, particle size decrease. As in Table (4.1) prepared catalysts have smaller particle size than commercial catalysts, with smaller E_g values. Moreover, this is important for bacterial deactivation. Prepared catalyst is considered more efficient due to having smaller particles and larger relative surface area available for deactivation process.

4.2.2. Electronic Absorption Spectra.

Electronic Absorption Spectrum was measured for naked commercial and prepared ZnO, and for commercial and prepared ZnO/Anthocyanin catalyst suspensions. Fig. (4.2) shows the spectrum and maximum wave length (nm) for each of these materials.

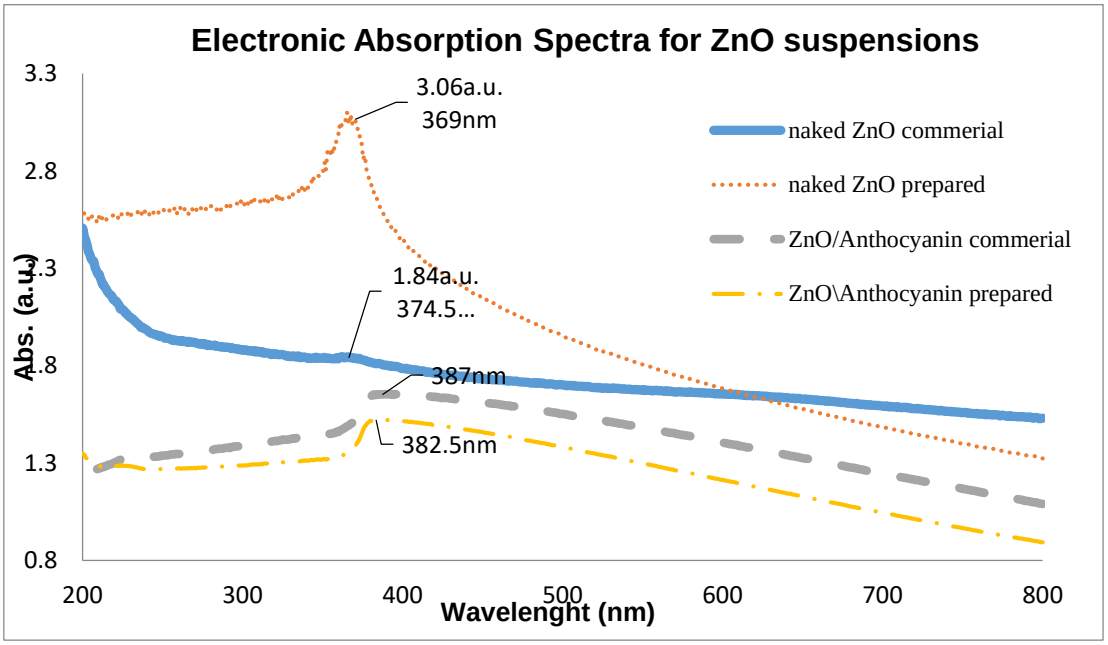

Figure (4.2): UV-VIS absorption characteristics of ZnO NPs systems dispersed in 50 mL distilled water.

As shown in Fig. (4.2) prepared ZnO NPs give absorbance peak at (369 nm). Compared with commercial ZnO (374.5nm), the prepared catalyst has smaller size. These results are consistent with literature [82]. On the other hand, absorptivity` indicates ability of the catalyst in absorbing incident photons, with high absorptivity of prepared ZnO reach (3.06 a.u.) compared to commercial catalyst (1.843 a.u.). Prepared ZnO is thus expected to be more efficient in photo- mineralization reaction due to its ability to absorb photons than other systems. Its ability in bacterial deactivation is expected to higher.

For sensitized systems no absorption band appeared in region (530-560) nm related to Anthocyanin dye [83]. As a result, only little Anthocyanin dye molecules were stuck on catalyst surface where the color of white powder catalyst was converted to purple after sensitization process.

4.2.3. SEM Results.

Both naked commercial and prepared ZnO were studied using Scanning Electron Microscopy. This was to study particle nature and morphology. The results are shown in Fig. (4.3):

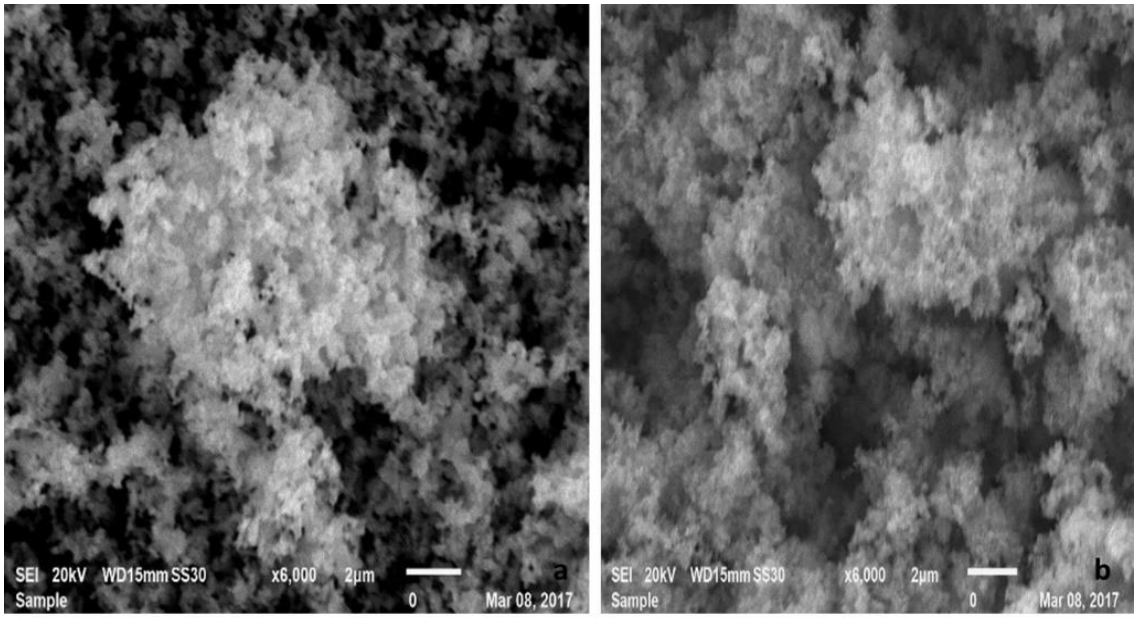

Figure (4.3): SEM images for solid ZnO powders (a) commercial, (b) prepared.

The Fig. (4.3) shows agglomerates of (rice shape). The pictures confirm the formation of ZnO NPs and approximate spherical shape of nanoparticles inside the agglomerates. Each agglomerate involves a number of nano-size ZnO particles bound together. By comparing two powder SEM images, prepared ZnO has smaller particle or agglomerate size than commercial powder. This means that synthetic ZnO has more surface area and its catalytic efficiency in bacterial deactivation will be higher.

4.2.4. XRD Results.

The average crystallite sizes of the samples were calculated by Debye Scherrer's equation $D_P=0.94\lambda\backslash\beta\cos\theta$, using the full width at half maximum of the X-ray diffraction peaks Where, Dp = Average Crystallite size, β = Line broadening in radians, θ = Bragg angle, λ = X-Ray wavelength [65]. As in Fig. (4.4) XRD patterns for both commercial and prepared ZnO NPs were studied.

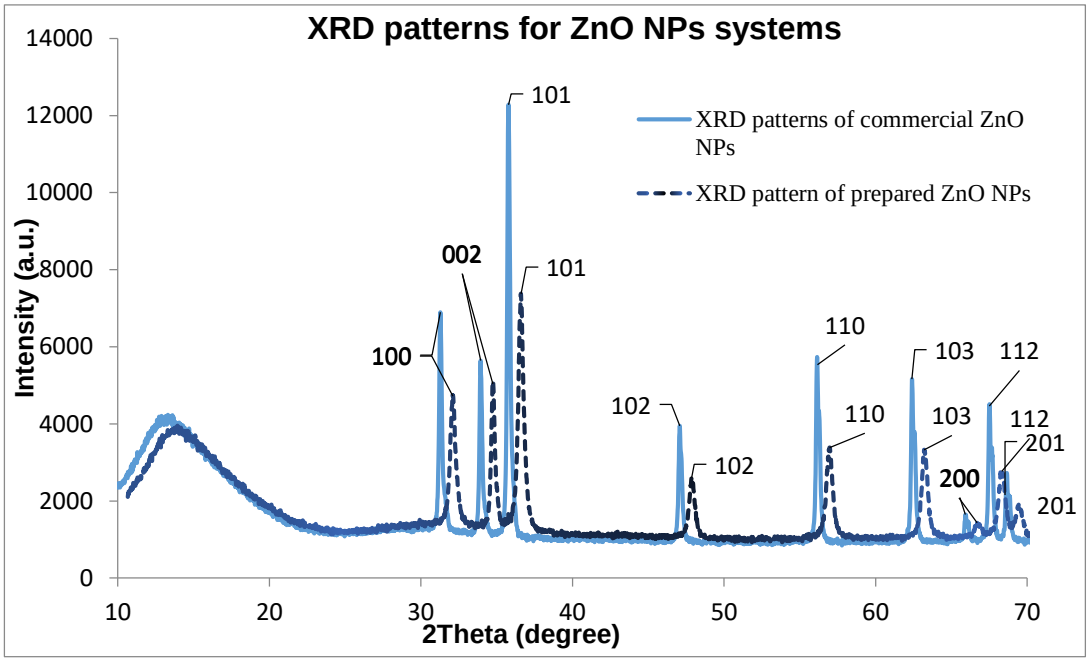

Figure (4.4): XRD patterns for ZnO NPs systems**.**

As in Fig. (4.4) all the diffraction peaks are well indexed to the hexagonal ZnO wurtzite structure [45]. Diffraction peaks corresponding to possible impurity were not found in the XRD patterns, confirming the good purity of the synthesized ZnO as it did not contain any XRD peaks for other than ZnO peaks. Moreover, the line broadening of the XRD peaks indicates that both ZnO powders consist of particles in nanoscale.

Table (4.2) summarizes Crystallite size in D (nm) for both commercial and prepared catalysts. Based on Debye Scherrer's equation [65].

Table (4.2): Average crystallite size of commercial and prepared ZnO calculated by XRD.

X-ray diffraction peaks	Crystallite size, D(nm) for commercial ZnO	Crystallite size, D(nm) for prepared ZnO
(100)	32.07	13
(002)	33.34	21.62
(101)	32.84	19.56
(102)	24.34	9.69
(110)	23.6	11.81
Average	29.24	15.136

Table (4.2) shows that average crystallite size for commercial catalyst was (29.24 nm) and for prepared catalyst was(15.136nm). Smaller size means higher surface area of catalyst which increases its efficacy in disinfection of polluted water. By these results we expect that prepared catalyst will be more efficient than commercial catalyst in deactivating bacteria. Both SEM and XRD results summarize the particle size for both ZnO systems. Both SEM and XRD results show that prepared ZnO powder has smaller crystallite size (15.136 nm) than commercial ZnO (29.24 nm).

4.2.5. UV-Visible Spectra for Anthocyanin dye.

Fig. (4.5) shows absorption spectrum of the concentration of Anthocyanin dye after and before used in sensitization process for commercial and prepared ZnO NPs:

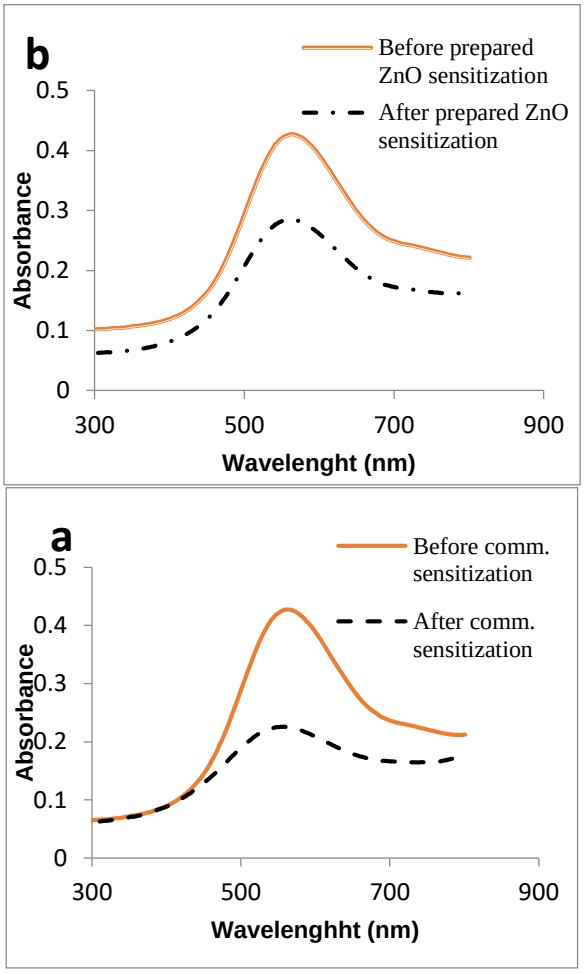

Figure (4.5): Absorption spectrum, a graph of absorbance vs. wavelength(nm) in ethanol for the concentration of Anthocyanin dye after and before used (a) commercial ZnO sensitization, (b) prepared ZnO sensitization.

By using the Electronic Absorption Spectrum [46, 81], dye concentration can be determined. Using Beer-Lambert law for absorbance, $\mathbf{A} = \boldsymbol{\varepsilon} \times \mathbf{l} \times C$

* Where, **A** is the amount of light absorbed by Anthocyanin. **A** is highest value of absorbance taken from Absorption spectrum graphs in Fig. (4.5).

* **ε** is the molar absorptivity. For Anthocyanin dye= 7.11×10^4 $m^2.mol^{-1}$.

* **l** is the distance that the light travels through the solution = 78.5×10^{-4} m^2.

*C is the concentration of the absorbing species per unit volume.

Table (4.3) summarizes the concentrations of Anthocyanin before and after using it in sensitization of ZnO systems. Number of dye molecules attached onto catalyst particles was then calculated. Number of molecules per Zn atom was then calculated for each sensitized catalyst system.

Table (4.3): Concentrations of Anthocyanin dye before and after supporting on ZnO powders.

Anthocyanin dye	Concentration (mol\L) $\times 10^{-5}$	Dye Molecules /Atom Zn
Before prepared ZnO sensitization	75	0.5×10^{-5}
After prepared ZnO sensitization	40	
Before commercial ZnO sensitization	76.5	0.293×10^{-5}
After commercial ZnO sensitization	56	

As in Table (4.3) the dye amount taken by prepared ZnO NPs was more than commercial ZnO. As shown before by PL, SEM and XRD results, prepared catalyst has smaller size than commercial. As a results, the efficiency of dying process on prepared catalyst will be higher, as confirmed by Table (4.3) results. 0.5×10^{-5} molecule of dye was absorbed per one atom of prepared Zn. This is higher than in commercial catalyst which absorbed 0.29×10^{-5} molecule dye for one Zn atom. Anthocyanin is expected to increase the catalyst ability to produce extra free radicals in the visible region. As a result, catalyst with more dye more values will be more efficient in bacterial disinfection in the visible range.

4.3 Simulated Solar Irradiation Experiments.

Both naked ZnO and ZnO/Anthocyanin catalysts were used against G +ve *S. aureus* and –ve *K. Pneumonia* bacteria under solar simulated radiations. Performances of both catalysts were found and compared together with QY, TF and deactivation percent which are simply calculated by following methods [47]:

✓ Quantum Yield (QY):

$$QY = \frac{\text{Number of bacterial colonies found experimentally}}{\text{Number of incident photons (n)}}$$

Where n,

$$n = \frac{E \times \lambda}{C \times h}$$

Where, (E) Energy, (λ) Wavelength, (C)Speed of light, (h)Planck's constant.

$$Energy = Watt\ per\ area \times Time\ per\ second.$$

✓ Turnover Number (TN):

$$TN = \frac{Number\ of\ deactivated\ bacteria}{Atoms\ of\ ZnO}$$

$$TF = \frac{TN}{Time}$$

✓ $Deactivation\ percent = [\frac{No.of\ deactivated\ bacteria}{No.of\ initial\ bacteria}] \times 100\%$

4.3.1. Impact of time on bacteria deactivation.

Fig. (4.6) illustrates the influence of exposure time on the deactivation percentage of (1×10^6 CFU\mL) of both G +ve *S. aureus* and G -ve *K. pneumoniae* bacteria treated by 0.1 g of (both naked and sensitized ZnO) in separate experiments under light.

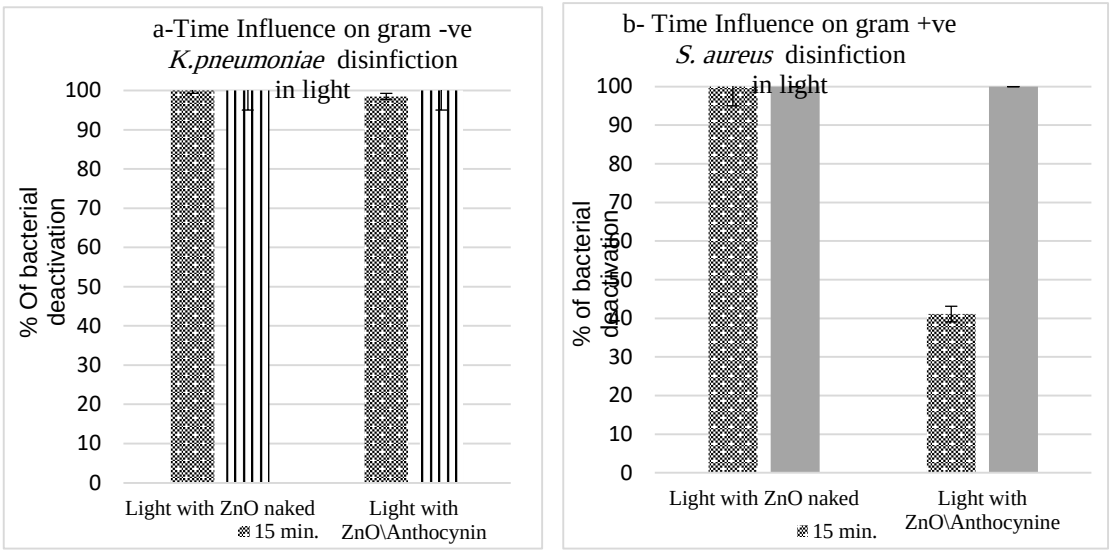

Figure (4.6): Influence of exposure time on the deactivation percentage of (1×10^6 CFU\mL) bacteria, catalyst loading 0.1 g at 30 ºC under light (a) *K. pneumonia* bacteria, (b) *S. aureus* bacteria.

Fig. (4.6) shows that after 60 min all bacteria (*K. pneumonia*e bacteria and *S. aureus* bacteria) were completely deactivated. Therefore, shorter exposure time (15 min) was necessary to compare the effectiveness of naked and sensitized ZnO systems. The deactivation percent of naked ZnO was still 100% compared to ZnO\Anthocyanin which declined to only 43% after 15 min for *S. aureus* treatment. The deactivation percent of *K. pneumoniae* bacteria treated with two catalysts was almost the same after 15 min. Unexpectedly, Anthocyanin dye lowered the efficiency of ZnO particles against *S. aureus* bacteria. This could be due to screening effect of Anthocyanin dye particles on active sites of ZnO, and shielding them away

from incident light. So ZnO efficiency toward bacteria decreased when using the dye.

Fig. (4.7) shows the influence of exposure time on the deactivation percentage of (1×10^6 CFU\mL) of both G +ve *S.aureus* and G -ve *K. pneumoniae* bacteria using0.1 g of (both naked or sensitized ZnO) in separate dark experiments.

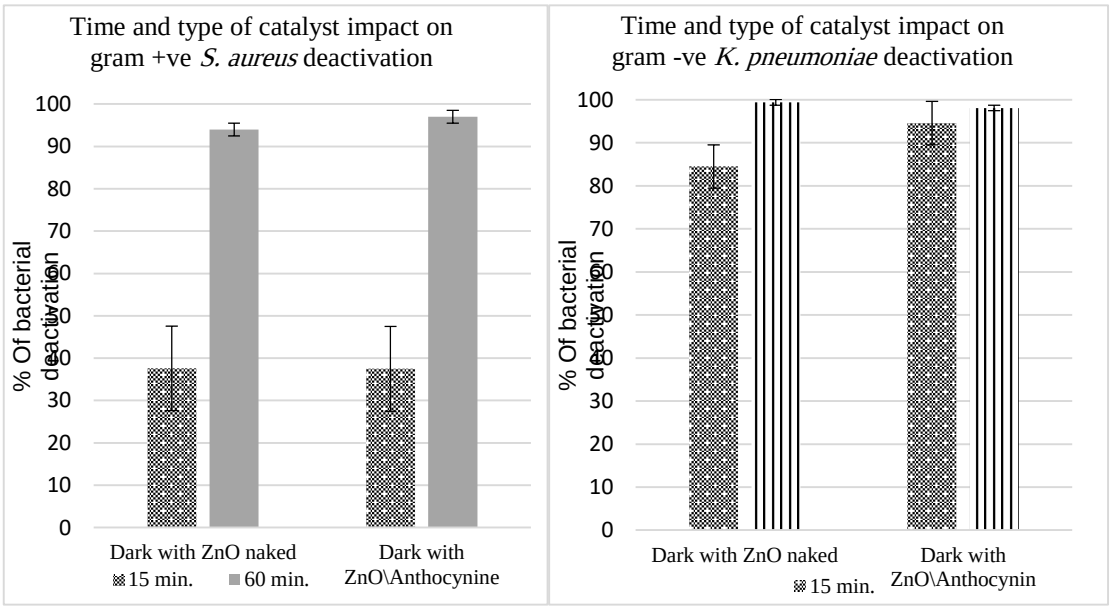

Figure (4.7): Influence of exposure time on the deactivation percentage of (1×10^6 CFU\mL) bacteria, catalyst loading 0.1 g at 30 ºC in dark (a)*K. pneumonia* bacteria, (b)*S. aureus* bacteria.

As shown in Fig. (4.7) the deactivation percent was still high between (100 -91) % for both bacteria after 60 min. The percent decreased to ~ 37% for both catalysts in dark experiments for G +ve *S.aureus* after 15 min, whereas deactivation for G -ve *K. pneumoniae* is still high in dark with percentages around 90%. Detailed mechanism in dark for ZnO NPs work is still not known yet. Most widely accepted mechanism assumes changing in bacterial

membrane permeability and dissipation as a result of accumulation and attachment of ZnO NPs on the bacterial membrane [67, 74].

Tables (4.4, 4.5) summarize values of quantum yield (QY), turnover frequency (TF) and deactivation percent of (1×10^6 CFU\mL) of both *S. aureus* and *K. pneumoniae* bacteria using 0.1 g of naked ZnO in light and dark for (15, 60) min.

Table (4.4): Values of QY, TF and deactivation percent for different exposure times. All experiments were done using 0.1 g of naked ZnO against S.aureus (1×10^6 CFU\mL) at 30ºC.

	No. of deactivated Bacteria (CFU\mL)×10^6		QY ×10^{-15}		TF (min^{-1})×10^9		% Of bacterial deactivation	
Time (min.)	15	60	15	60	15	60	15	60
ZnO in light	0.21	0.03	0.15	0.005	0.01	0.0004	100	100
ZnO in dark	0.16	0.53	0.11	0.094	0.01	0.0071	37.6	94
Light only	0.78	0.97	0.56	0.175	0.04	0.013		
Dark only	0.58	0.44	0.42	0.079	0.03	0.006		

Table (4.5): Values of QY, TF and deactivation percent for different exposure times. All experiments were done using 0.1 g of naked ZnO against K. pneumoniae (1×106 CFU\mL) at 30ºC.

	No. of activated bacteria (CFU\mL)$10^{\wedge 6}$		QY×$10^{\wedge -15}$		TF (min^{-1}) ×$10^{\wedge 9}$		% Of bacterial deactivation	
Time(min)	15	60	15	60	15	60	15	60
ZnO in light	0.57	0.017	0.41	0.031	0.031	0.00	100	100
ZnO in dark	0.36	0.98	0.255	0.176	0.019	0.013	84.5	99
Light only	0.43	0.982	0.31	0.33	0.023	0.013		
Dark only	0.58	0.01	0.42	0.032	0.031	0.002		

Tables (4.4, 4.5) show that OY and TF values. They were higher at the beginning of treatment, due to higher bacterial concentrations, which promoted more deactivation for both bacteria types. However, as the reaction proceeded, bacterial concentration was lowered which caused decrease in the deactivation percent per time unit. Another reason is also possible. As reaction progressed, organic molecules resulting from deactivated bacteria will become higher and catalyst functioned to decompose both these organic molecules and the remaining survived bacterial cells.

Both bacteria showed small resistance when treated with ZnO NPs meaning after 60 min as both bacteria were completely deactivated (100% deactivation) in light and dark as shown in Figs. (4.6, 4.7). After 15 min in dark *S.aureus* showed more resistance than *K.pneumonia,* because *S.aureus's* cell membrane is thicker than *K. pneumoniae* 's membrane and *S.aureus* survived better in dark.

4.3.1.a-TOC Results

By oxidizing organic carbon output from deactivated bacteria, the Total Organic Carbon could be detected and quantified by calculating the amount of oxidized carbon (CO_2). As shown in Table (4.6) samples from mineralization experiments (using 0.1g of naked ZnO) separately against (1×10^6 CFU\mL) of *S. aureus* and *K. pneumonia* were taken after 3 hrs treatment.

Table (4.6): TOC results for bacterial aqueous mixtures remaining from experiment after 3 hrs treatment with 0.1 g of naked ZnO against (1×10^6 CFU\mL) of both *S. aureus* and *K. pneumonia* in light and dark at 30 ºC.

TOC value (mg/L)				
	S. aureus		*K. pneumonia*	
	With ZnO	Without ZnO	With ZnO	Without ZnO
Light	0.634	49.84	29.74	54.23
Dark	39.25	39.5	40.09	39.25

Table (4.8) shows that for *S. aureus* experiments a clear decrease in organic carbon occurred in light. The waste water treated with naked ZnO showed TOC value0.634 mg\L compared to the sample without catalyst which showed 49.84 mg\L for TOC (98.7% of organic matter were mineralized). This big difference between the two values confirms that ZnO not only deactivates bacteria, but also mineralizes their organic matters. However, in dark, the TOC analysis gave almost the same TOC value~ 39 mg\L with and

without using naked ZnO. The ability of ZnO catalyst in dark to form free radicals is not possible.

On the other hand, TOC for aqueous mixtures of *K. pneumonia* bacteria treated in light, with naked ZnO, was 29.7 mg\L decreasing roughly to the half of the value of bacteria without treatment which 54.2mg\L (45.2% of organic matter were mineralized). This means that after 3 hrs ZnO deactivated all *K. pneumonia* bacteria, and partly mineralized them into minerals and gases. While treatment in dark did not give significant difference in values of TOC. This means that ZnO deactivated bacteria without mineralization, in the dark. TOC results for control samples (without catalyst) in light and dark condition for *K. pneumonia* show that organic matter in dark is less than in light. This is because *K. pneumonia* bacteria grows in dark more than in light, causing more consumption of water organics. So less organics were found in dark.

4.3.2. Cutting off UV-light experiment.

Cut-off experiments were made to distinguish between activities of naked and sensitized ZnO particles. A light cut off filter to exclude 400 nm and shorter (UV light) was used. As a result, the bacteria were treated under visible light only. ZnO/Anthocyanin activity should function in case of visible light with cutting off filter. The naked ZnO NPs should show some decrease in the catalytic efficiency with cutting off the UV light. As shown in Fig. (4.8) cutting off experiments were done by using 0.1g of naked ZnO

or 0.1g of ZnO\Anthocyanin in two separate experiments against (1×10^6 CFU\mL) of both *S.aureus* or *K. pneumoniae* bacteria for 15 min.

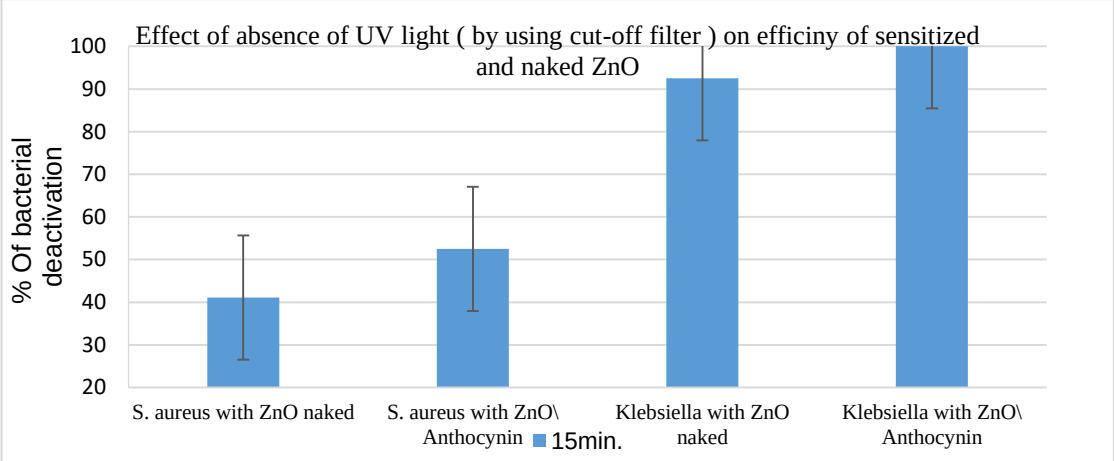

Figure (4.8): Bacterial deactivation using solar simulated light with a cut-off filter. Experiments were conducted using 0.1g of naked ZnO or 0.1g of ZnO\Anthocyanin in two separate experiments against ($1*10^6$ CFU\mL) of both *S.aureus*or *K. pneumoniae* bacteria at 30 ºC.

Fig. (4.8) shows, *S.aureus* deactivation percent decreased from 100% (by naked ZnO NPs without filter) to 41% (with filter). This shows the importance of ~5% of UV region present in sun light simulator and its effect on ZnO efficiency. On the other hand, the deactivation percentage of the same bacteria treated with ZnO\Anthocyanin was 42% without cut-off filter, and 52% with cut-off filter.

However, for *K. pneumoniae* treatment no big difference appears between the efficiency of two catalysts in cut- off experiments. Deactivation percent by using naked ZnO was (92.5%) compared to ZnO\Anthocyanin (99%) after 15 min. This means that Anthocyanin dye did not make high impact on ZnO work in photo-mineralization against biological pollutants under visible light.

4.3.2.a-TOC results in cutting-off experiment for G +ve *S. aureus*.

To study impact of visible light only, three beakers with 50 mL water polluted with 1×10^6 CFU\mL *S. aureus* bacteria were exposed to visible light with wavelengths longer than 400 nm for 3 hrs. A cut-off filter was used for this purpose. The first beaker was treated with 0.1g naked ZnO, the second with 0.1g ZnO\Anthocyanin and the third without catalyst. All beakers contained bacterial solution with same concentration. The results of cutting off UV-Light experiment are shown in Table (4.7).

Table (4.7): Total Organic Carbon calculated in cutting off UV-Light experiment of 1×10^6 CFU\mL *S. aureus* mineralized by 0.1g of catalyst, at 30 ºC for3 hrs.

Without catalyst(mg\L)	With 0.1g ZnO\Anthocyanin(mg\L)	With 0.1g naked ZnO(mg\L)
52.25	54.97	57.98

After 3 hrs, TOC results in Table (4.7) showed that both naked and sensitized catalysts could not mineralize organic matters coming from deactivated bacteria. All experiments showed comparable TOC values of low mineralization for organic molecules. The results mean that ZnO cannot form radicals necessary to mineralize organic stuff. Sensitization of ZnO with Anthocyanin dye should increase the catalyst ability to form radicals, but the results do not confirm that ZnO\ Anthocyanin cannot form radicals to mineralize deactivated bacterial contents.

4.3.3. Impact of naked ZnO catalyst loading.

lowering the loading of naked ZnO is necessary for practical and economic reasons. Impacts of this reduction on the deactivation percentage of 1×10^6 CFU\mL (*S. aureus* and *K. pneumonia*e) in light and dark were studied. Fig. (4.9) shows the results.

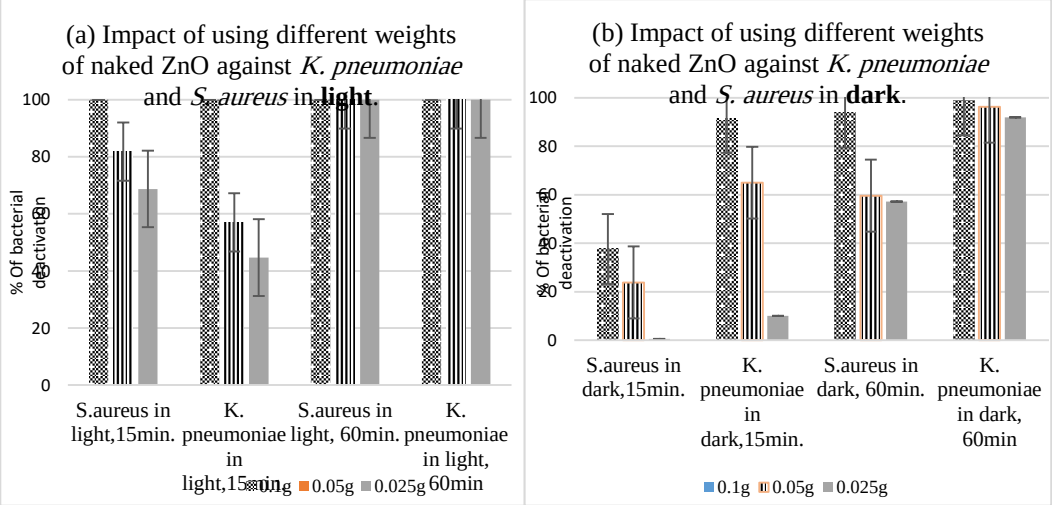

Figure (4.9): Impact of catalyst loading on the deactivation percentage of *S. aureus* and *K. pneumonia* (1×10^6 CFU\mL) after (15, 60) min at 30 ºC in (a) light, (b) dark.

Fig. (4.9) shows that in light and dark, after 60min almost all bacteria (*S. aureus* and *K. pneumonia*e) were deactivated by using 0.025g of naked ZnO. However, deactivated percentages were lowered after 15 min to (81.8%, 68.7%) and (57%, 44.7%) when 0.05g and 0.025g of ZnO were used against *S.aureus* and *K. pneumoniae*, respectively. By reducing the catalyst's weight from 0.1 g to 0.025g catalyst can still remove more than half of bacterial concentration found in water in15 min. This is good advantage for naked ZnO efficiency.

In dark after 15 min for both *S.aureus* and *K.pneumonia* bacteria, reducing catalyst weight extremely impacted deactivation percent. The percentage values ranged between ~ (48 - 5) %. This decrease is due to short treatment time (15 min is not enough period for catalyst to deactivate in dark). However, bacterial deactivation in dark is due to the redistribution of the cell's metabolic system by ZnO NPs as explained in literature. [66-74]. Tables (4.8, 4.9) show values of QY, TF and deactivation percent calculated for experiments tested using different naked ZnO loads against 1×10^6 CFU\mL of (*S. aureus* and *K.pneumonia*e) in light after 15 min.

Table (4.8): Values of QY, TF and deactivation percent, for experiments with different naked ZnO loading against 1×106 CFU\mL of S. aureus in light after 15 min.

Catalyst loading (g)	No. of leactivated bacteria (CFU\mL)×10^6	Q Y×10^{-15}	TF (min^1)×10^9	% Of bacterial deactivation
0.10	0.214	0.154	0.011	100
0.05	0.175	0.126	0.020	81.8
0.025	0.147	0.11	0.031	68.7

Table (4.9): Values of QY, TF and deactivation percent for experiments with different naked ZnO loading against 1×10^6 CFU\mL *K. pneumoniae* in light after 15 min.

Catalyst loading (g)	No. of deactivated bacteria (CFU\mL) ×$10^{\wedge6}$	QY×$10^{\wedge-15}$	TF (min^{-1}) ×$10^{\wedge9}$	% Of bacterial deactivation
0.10	0.57	0.41	0.031	100
0.05	0.324	0.232	0.035	57
0.025	0.255	0.183	0.055	44.7

As in Tables (4.8 and 4.9) for both bacteria types, increasing catalyst loading showed higher deactivation percent. This by giving more active sites and

higher total surface area of catalyst for bacterial deactivation. In Tables (4.8 and 4.9) QY values increase as catalyst weights increase with (0.154×10^{-15}, $0.126\times10^{-15)}$, 0.11×10^{-15}) and (0.41×10^{-15}, 0.232×10^{-15}, 0.183×10^{-15}) when 0.1, 0.05 and 0.025 Gs were used against *S.aureus* and *K. pneumonia*e bacteria, respectively. As catalyst loading increased more photons are used for deactivation.

Tables (4.8 and 4.9), show that TF values decreased as catalyst weights increased. This means that relative efficiency of the ZnO catalysts decreased with higher loading. This is presumably to tendency of ZnO particles to screen each from UV light.

4.3.4. Impact of bacterial concentration.

Impact of bacterial concentration of both *S.aureus* and *K.pneumonia*e on bacterial deactivation was studied using 0.1 g naked ZnO in treatment process. In Fig. (4.10), 0.1g of naked ZnO was used to treat different concentrations of *S.aureus* and *K. pneumonia*e bacteria in separate experiments in light or dark for 60 min at 30ºC.

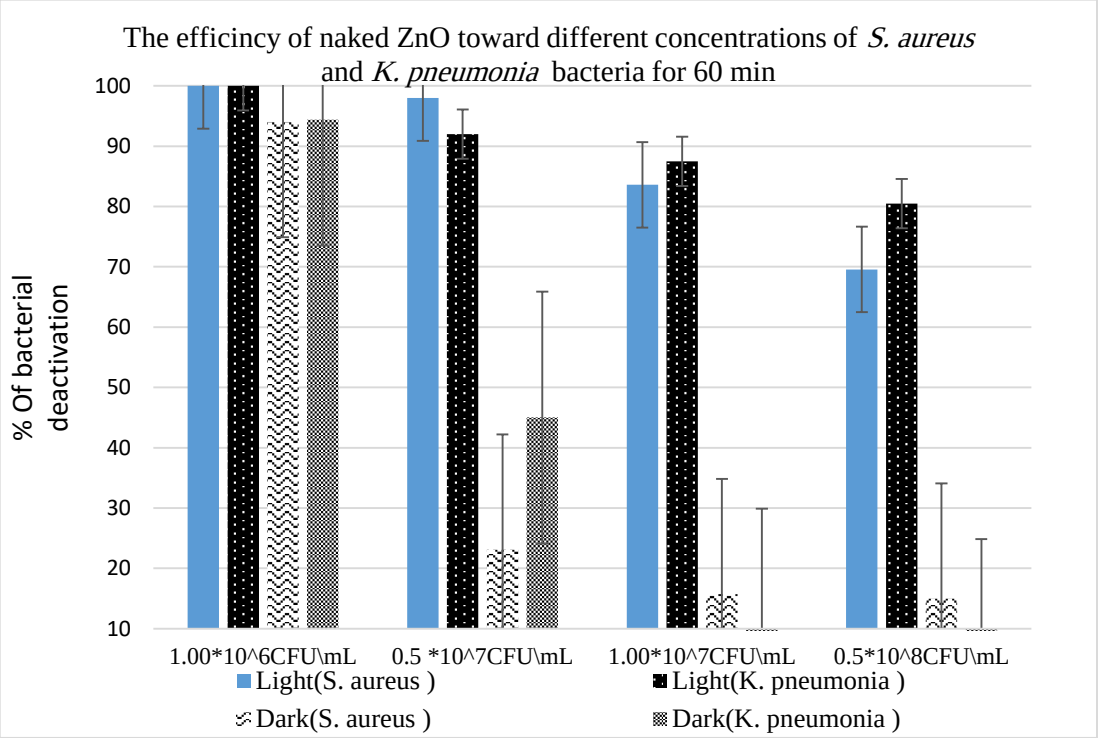

Figure (4.10): Impact of increasing the concentrations of *S.aureu* sand *K. pneumonia* bacteria on the deactivation percentage using 0.1 g of naked ZnO in light or dark for 60 min at 30ºC.

Fig. (4.10) shows that when the concentrations of both *S. aureus* and *K. pneumonia*e bacteria increase the deactivation percentages decrease.

The results show that under light 69.56% and 80.5% of *S.aureus* and *K. pneumonia*e, respectively, are deactivated in 60 min, from 0.5 $\times 10^8$ CFU\mL. The results are encouraging; as high concentrations are used. On the other hand, in dark when bacterial concentrations became extremely high the ZnO NPs efficiency disappeared and deactivation percent reached only 15%of 0.5 $\times 10^8$ CFU\mL of *S. aureus*.

Tables (4.10 and 4.11) illustrate values of QY, TF and deactivation percent related to increasing bacterial concentrations of both (*S. aureus* and *K. pneumonia* bacteria) using 0.1 g of naked ZnO in light for 60 min.

Table (4.10): Values of QY, TF and deactivation percent of increasing the concentrations of *S.aureus* using 0.1 g of naked ZnO in light after 60 min at 30ºC.

Bacterial concentration (CFU\mL)	No. of deactivated bacteria (CFU\mL)×10^5	Q Y×10^{-16}	TF (min^{-1})×10^8	% Of bacterial deactivation
1.0×10^6	0.031	0.0056	0.0042	100
0.5×10^7	4.52	0.81	0.061	98.1
1.0×10^7	15.05	2.7	0.2	83.61
0.5×10^8	80.3	14.4	1.1	69.56

Table (4.11): Values of QY, TF and deactivation percent of increasing the concentrations of *K. pneumonia* using 0.1 g of naked ZnO in light after 60 min at 30º C.

Bacterial concentration (CFU\mL)	No. of deactivated bacteria(CFU\mL)×$10^{\wedge 5}$	QY×$1^{0\wedge -16}$	TF (min^{-1})×$10^{\wedge 8}$	% Of bacterial deactivation
1.00×10^6	0.172	0.031	0.0023	100
0.50×10^7	3.49	0.63	0.047	92
1.00×10^7	4.05	0.73	0.055	87.5
0.50×10^8	3.06	0.55	0.025	80.5

Tables (4.10 and 4.11) show that increasing in initial bacterial concentration increases the values of QY and TF. When bacterial concentration increases, more bacterial cells are deactivated on the catalyst surface and more bacterial cells are lost. Even for lower deactivation percentage. The relative efficiency of 0.1 g of catalyst increases with increasing initial bacterial concentrations.

4.3.5. Impact of Temperature on photo-mineralization reaction.

Different Temperatures do not impact ZnO\Anthocyanin works against bacteria. Temperatures (20ºC, 27ºC, 37ºC) did not impact the catalyst efficiency [48]. Temperatures (26,28,30,32,34,36,38 ºC) were tested on naked ZnO [49].

For *S.aureus* bacteria, the suitable Temperature range for growth is between 7 to 48°C, with an optimum at 37°C [52]. However, reduction in the growth of *K. pneumonia* bacteria happened at Temperatures >37 °C and their ideal growth Temperature was 25° to 37° [50,75]. Literature thus confirm that within the range (20-37 ºC), the Temperature does not have impact on bacterial deactivation. In this work, the Temperature 30 ºC was used for technical reasons. Due to exposure to light, water temperature stabilizes at 30 ºC (slightly higher than room Temperature 25 ºC). For this reason, we used the 30 ºC at which solution Temperature stabilized.

4.3.6. Impact of pH on catalyst efficiency.

Different values of pH did not impact ZnO\Anthocyanin catalyst. This is reported in literature [48] where (5.0, 7.5, 8.7) pH values showed no impact on the catalyst efficiency. Different values of pH (4.50, 7.04, 9.00) tested on the naked ZnO efficiency showed no difference [49]. For *S.aureus* bacteria growth occurred over the pH range of 4.0–10.0, with an optimum at 6–7 [52].For *K. pneumonia* bacteria growth, the ideal pH level is about 7.2 [51].Changing of water pH values within the ranges exist in nature, will thus

not affect the bacterial growth or the efficiency of mineralization process. Thus, the pH value used in all experiments here was 7.05.

4.3.7. The impact of stirring type.

As shown in Table (4.12) three types of stirring: medium magnate stirring, shaking and no stirring were examined at dark condition for 30 min with treated 2.01×10^5 CFU\mL of *K. pneumonia* bacteria using 0.1 g of naked ZnO.

Table (4.12): Impact of stirring type on the efficiency of deactivation 2.01×10^5 CFU\mL of *K. pneumonia* bacteria in dark with 0.1g of naked ZnO after 30 min at 30 ºC.

Concentrations of growing bacteria (CFU\mL)			
	Magnetic stirring	Shaker	No stirring
With ZnO naked	0.00	0.00	14×10^3
No catalyst (control sample)	1.25×10^3	5.00×10^3	132×10^3
Bacterial deactivation percent	100	100	89.4

As in Table (4.12) shows highest efficiency for magnetic stirring. *K. pneumonia*e considered as anaerobic bacteria [53] that it need no O_2 to grow. By magnetic stirring and shaking it gains more O_2 by moving solution. However, the magnetic stirring and shaking movement gave an excellent performance with complete deactivation of bacteria by ZnO. For practical purposes, shaking is the best to follow. Shaking of polluted water can be achieved either with shaker or by natural motion (streams). Without motion

bacteria dose not quickly reach ZnO surface effectively. Therefore, lower deactivation percentage is observed in case of no stirring.

4.3.8. Catalyst recycling.

In catalyst recycling experiments both naked ZnO or ZnO\Anthocyanin were reused for 3rd time against 1×10^6 CFU\mL of *S. aureus* bacteria each time for 60 min in light or in dark. At the end of the first run and after autoclaving the treated sample (to make sure all bacteria were deactivated) the catalyst was recovered and reused. The remains of 0.1 g of the catalyst were taken and washed several times with distilled water, to remove all possible organics. Then 50 mL of distilled water were added to the recovered catalyst. Bacteria were added as described for fresh catalyst sample as shown before, and the catalyst was ready for reuse. Fig. (4.11) shows the catalyst recycling for 3rd time working on *S.aureus* treated with 0.1 g of naked ZnO.

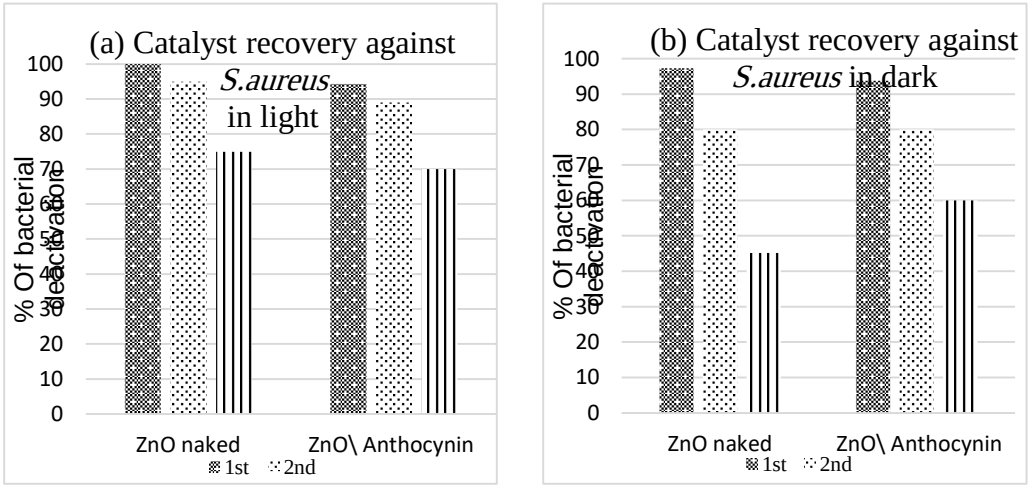

Figure (4.11): 0.1 g of naked ZnO or 0.1g of ZnO\Anthocyanin were reused for 3rd time against of *S. aureus* (1×10^6 CFU\mL), for 60 min. at 30 ºC (a) in light, (b) in dark.

Fig. (4.11) shows possibility to reuse the catalyst for third time in light or in dark, with deactivation percent lowering to 71% for ZnO\Anthocyanin and 75% for naked ZnO in light. In dark, lowering to 60% for ZnO\Anthocyanin and 45% for naked ZnO are observed. Some of catalyst amount was lost during washing and decantation process, so the relative deactivation percent is not significant. Mass of recovered ZnO was calculated for fresh sample (0.1 g), first recovered sample (0.093 g) and second recovered sample (0.073 g). relative activity (number of deactivated bacteria / grams of ZnO) was then calculated for each case. Relative activity remained constant for fresh catalyst, first recovered and second recovered. The values in light were (0.22×10^8 per gram) in each case and in dark were (0.44×10^9 per gram) for ZnO systems. For ZnO\Anthocyanin, the values were (0.21×10^8 per gram) in light and (0.38×10^9 per gram) in dark. The results show that the catalyst did not loss its efficiency on recovery for second recovery. This shows the value of using the ZnO catalyst systems for water disinfection.

Conclusion and Recommendations:

The results show that ZnO NPs can be effective catalyst to deactivate G +ve *S. aureus* and G -ve *K. pneumoniae* bacteria in both dark and light experiments. Under light, mineralization bacteria occur for *S. aureus* (99%) and *K. pneumonia*e (45%), for the first time. ZnO catalysts can also be recovered and reused for second time without loss of relative activity. The results show the potential of using ZnO catalyst system in future waste water disinfection. For future work, we suggest applying the ZnO catalyst against other types of bacteria and other species such as viruses and algae. In

addition to, studying the impact of presence some ions inside water which may increase the turbidity such as Ca^{2+} and Mg^{2+} ions and its effect on the water disinfection. Moreover, applying the ZnO catalyst on sewage water, in cooperation with the Water Authority. The study should involve both organic contaminants and microorganisms. Finally, this project could be applied by create filter models which consist of ZnO insoluble powder, shaped as discs and used as water faucet filter.

Results show that water disinfection from both types of G + and G- bacteria can be achieved using direct solar light with safe, economic and available nano- ZnO catalyst. In addition to killing the bacteria, total mineralization of their organic content can be achieved, therefore, using the described strategy in Palestine and other countries, in addition to, Pilot plant study on naturally polluted water is highly recommended.

References

1. Social Media Pack, ***2.1 billion people lack safe drinking water at home, more than twice as many lack safe sanitation***, Available at: http://www.who.int/mediacentre/factsheets/fs391/en/ accessed in 3rd June 2017.
2. A. Morishima, ***International Review for Environmental Strategies, the Institute for Global Environmental Strategies***, **Institute for Global Environmental Strategies**, 6:229 – 250, 2006.
3. World Health Organization, ***Guidelines for drinking-water quality [electronic resource]: incorporating first addendum***,1:154-696, 2006.
4. B. Oram, ***Radiological Contaminants***, Available at: http://www.water-research.net/index.php/radiological-contaminants, accessed in 4th June 2017.
5. ***Guidelines for Drinking-water Quality***, Available at: http://apps.who.int/iris/bitstream/10665/44584/1/9789241548151_eng.pdf CH9, accessed in 4th June 2017.
6. ***Adolescents: health risks and solutions***, Available at: http://www.who.int/mediacentre/factsheets/fs391/en/ (UNDP, 2006, accessed in 4th June 2017.
7. R. Móra , R. Amann, ***Past and future species definitions for Bacteria and Archaea***, **Systematic and Applied Microbiology**, 38:209–216, 2015.
8. W. Navarre, O. Schneewind, ***Surface Proteins of G-Positive Bacteria and Mechanisms of Their Targeting to the Cell Wall Envelope***, **Microbiology and molecular biology reviews**,63:1174-229, 1999.

9. M. Mistou, I. Sutcliffe, N. Sorge, ***Bacterial glycobiology: rhamnose-containing cell wall polysaccharides in G-positive bacteria***, **FEMS microbiology reviews**, 40: 464-479, 2016.
10. I. Alexandraki, C. Palacio, ***G-negative versus G-positive bacteremia: what is more alarmin(g)?,*** **National Center for Biotechnology Information**, U.S. National Library of Medicine, 14:161, 2010.
11. N. Martinez, N. Ketheesan, G. Martens, K. West, E. Lien, H. Kornfeld, ***Defects in early cell recruitment contribute to the increased susceptibility to respiratory Klebsiella pneumonia infection in diabetic mice***, **Microbes and Infection**, 18:649-655,2016.
12. K. Okamoto , M. Lin , M. Haverkate , K. Lolans, ***Modifiable Risk Factors for the Spread of Klebsiella pneumonia Carbapenemase-Producing Enterobacteriaceae Among Long-Term Acute-Care Hospital Patients***, **Infection Control & Hospital Epidemiology**,38:670-677, 2017.
13. L. Gasink, P. Edelstein, E. Lautenbach, M. Synnestvedt, N. Fishman, ***Risk Factors and Clinical Impact of Klebsiella pneumonia Carbapenemase–Producing K. pneumoniae***, **Infection Control & Hospital Epidemiology**, 30:1180–1185, 2009.
14. R. Ainsworth, ***Safe piped water: Managing microbial water quality in piped distribution systems***, **World Health Organization**, Geneva, 2004, Available at: http://apps.who.int/iris/bitstream/10665/42785/1/924156251X.pdf, accessed in 11th June 2017.

15. J. Bartram, J. Cotruvo, M. Exner, C. Fricker, A. Glasmacher, ***Heterotrophic plate counts and drinking-water safety: The signifi cance of HPCs for water quality and human health***, **WHO Emerging Issues in Water and Infectious Disease Series**, 2003, Available at: http://www.who.int/water_sanitation_health/dwq/HPCFull.pdf, accessed in 11th June 2017.
16. Pathogen Safety Data Sheets: ***Infectious Substances – Staphylococcus aureus***, **Public Health Agency of Canada**, 2011, Available at: http://www.phac-aspc.gc.ca/lab-bio/res/psds-ftss/staphylococcus-aureus-eng.php, accessed in 11th June 2017.
17. M. Blaser, S. Falkow, ***ESSAY: What are the consequences of the disappearing human microbiota?***, **Nature Reviews Microbiology**, **7**: 887-894, 2009.
18. S. Antai, ***Incidence of Staphylococcus aureus, coliforms and antibiotic-resistant strains of Escherichia coli in rural water supplies in Port Harcourt***, **Journal of Applied Bacteriology**, 62:371–375, 1987.
19. M. LeChevallier, R. Seidler, **Staphylococcus aureus in rural drinking-water**, **Applied and Environmental Microbiology**, 39:739–742, 1980.
20. I. Sovadinova, P. Babica, O. Adamovský, A. Alpatová, V. Tarabara, B. Upham, L. Bláha, ***Chlorination and ozonation differentially reduced the microcystin content and tumour promoting activity of a complex cyanobacterial extract***, **Advanced in Oceanography and Limnology**, 8:4081, 2017.

21. *P. Cheung*, ***A Historical Review of the Benefits and Hypothetical Risks of Disinfecting Drinking Water by Chlorination***, **Journal of Environment and Ecology**, 8:2157-6092, 2017.

22. D. Dionysiou, G. Puma, J. Ye, J. Schneider, D. Bahnemann, ***Photocatalysis: Fundamentals and Perspectives***, **Royal Society of Chemistry**, London, 70-80, 2016.

23. A. Kołodziejczak-Radzimska, T. Jesionowski, ***Zinc Oxide—From Synthesis to Application: A Review***, **Materials**, **7**:2833-2881, 2014.

24. N. Padmavathy, R. Vijayaraghavan, ***Enhanced bioactivity of ZnO nanoparticles—An antimicrobial study***, **Science and technology of advanced materials**, 9:035004,2008.

25. S. Kumar, P. Venkateswarlu, V. Rao, G. Rao, ***Synthesis, characterization and optical properties of Zinc Oxide nanoparticles***,**International Nano Letters**, springer link, 3: 2228-5326,2013.

26. F. Delgado-Vargas, A. Jiménez, O. Paredes-López, ***Natural Pigments: Carotenoids, Anthocyanins, and Betalains — Characteristics, Biosynthesis, Processing and Stability***, **Critical Reviews in Food Science and Nutrition**, 40:173-289, 2010.

27. M. Merzlyak, O. Chivkunova, A. Solovchenko, K. Naqvi, ***Light absorption by anthocyanins in juvenile, stressed, and senescing leaves***, **Journal of Experimental Botany**, 59: 3903–3911, 2008.

28. K. Yoshida , M. Mori, T. Kondo, ***Blue flower color development by anthocyanins: from chemical structure to cell physiology***, **Natural Product Reports,** 26:884-915, 2009.

29. B. Subash, B. Krishnakumar, M. Swaminathan, M. Shanthi, ***Highly Efficient, Solar Active and Reusable Photocatalyst: Zr-Loaded Ag–ZnO for Reactive Red 120 Dye Degradation with Synergistic Effect and Dye-Sensitized Mechanism***, **American Chemical Society Publications**, 29:939–949, 2012.

30. M. Khatamian, , M. Fazayeli, B. Divband, ***Preparation, characterization and photocatalytic properties of polythiophene-sensitized zinc oxide hybrid nanocomposites***, **Materials Sciencein Semiconductor Processing**, 26:540–547,2014.

31. L. Saikia, D. Bhuyan, M. Saikia, B. Malakar, D. Dutta, P. Sengupta, ***Photocatalytic performance of ZnO nanomaterials for self- sensitized degradation of malachite green dye under solar light***, **Applied Catalysis A: General**,490:42-49, 2015.

32. D. Venieri, F. Tournas, I. Gounaki, V. Binas, A. Zachopoulos, G. Kiriakidis, D. Mantzavinos, ***Inactivation of Staphylococcus aureus in water by means of solar photocatalysis using metal doped TiO2 semiconductors***, **Journal of Chemical Technology and Biotechnology**,10:5085, 2016

33. B. Agarwal, T. Das, S. Baruah, ***Improvement of photocatalytic activity of Zinc Oxide nanoparticles using Zinc Sulphide Shell***, **ADBU-Journal of Engineering Technology**, 4:2348-7305, 2016.

34. J. Monteagudo, A. Duran, I. Martín, A. Acevedo, ***A novel combined solar pasteurizer/TiO2 continuous-flow reactor for decontamination and disinfection of drinking water***, **Chemosphere**, 168:1447-1456, 2017.

35. S. Lotfiman, M. Ghorbanpour, S. Lotfiman, M. Ghorbanpour, ***Antimicrobial activity of ZnO/silica gel nanocomposites prepared by a simple and fast solid-state method***, **Surface & Coatings Technology**, 310:129- 133, 2017.
36. S. El-Kacemi, H. Zazou, N.l Oturan, M. Dietze, M. Hamdani, M. Es-Souni, M. Oturan, ***Nanostructured ZnO-TiO2 thin film oxide as anode material in electrooxidation of organic pollutants. Application to the removal of dye Amido black 10B from water***, **Environmental Science and Pollution Research**, 24:1442–1449, 2017.
37. A. Kadam, T. Kim, D. Shin, K. Garadkar, J. Park, ***Morphological evolution of Cu doped ZnO for enhancement of photocatalytic activity***, **Journal of Alloys and Compounds**,710:102-113, 2017.
38. M. Ikhile, T. Barnard, J. Ngila, ***Potential application of synthesized ferrocenylimines compounds for the elimination of bacteria in water***, **Journal of Physics and Chemistry of the Earth**, 10:1-5, 2017.
39. S. Sutton, ***Measurement of Microbial Cells by Optical Density***, **Journal of Validation Technology**, 17**:**46-49, 2011.
40. S. Lacombe, T. Pigot, ***Materials for selective photo oxygenation vs. photocatalysis: preparation, properties and applications in environmental and health fields***, **Catalysis Science & Technology**, 6:571--1592, 2016.
41. N. Gilmour, R. Charles, ***"Water Treatment Using Advanced Oxidation Processes: Application Perspectives"***, **Electronic Thesis and Dissertation Repository**, The University of Western Ontario, **7**:836, 2012.

42. R. Milton, J. Salton, K. Shin Kim, ***Chapter 2. Structure***, **Medical Microbiology**, The University of Texas Medical Branch, Galveston,1996.
43. N. Hang, ***Photocatalytic application of metal oxide nanostructures***, For the Degree of Master of Philosophy at The University of Hong Kong, 2014.
44. J. Zhou, X. Zhao, ***Visible-Light-Responsive Titanium Dioxide Photocatalysts, Environmentally Benign Photocatalysts: Applications of Titanium Oxide-Based,*** **Materials**, 10:235-251, 2012.
45. P. Samadipakchin, H. Mortaheb, A. Zolfaghari, ***ZnO nanotubes: Preparation and photocatalytic performance evaluation***, **Journal of Photochemistry and Photobiology A: Chemistry**,337:91-99, 2017.
46. A. Robinson, ***How to Calculate Molar Absorptivity***, Available at: http://sciencing.com/calculate-molar-absorptivity-5161812.html, accessed 5th Aug 2017.
47. ***X-ray Photoelectron Diffraction (XPD) XPD – Science topic***, **Research Gate**, Available at: https://www.researchgate.net/post/How_to_calculate_the_turnover_number_of_a_catalyst, accessed 8th July , 2017.
48. S. Ateeq, H. Hilal, M. Dweikat, ***Water Disinfection by Photo-Degradation of Microorganisms Using Natural Dye-Sensitized ZnO Catalyst***, For the Degree of master at An-Najah National University, *2012*.
49. J. Ishtaiwa, M. Dwikat, S. Al-Shakhshir, ***Understanding Mode of Action of Nanoparticles in Water Disinfection: ZnO in Bacteria Killing vs. Complete Photo-degradation***, For the Degree of master at An-Najah National University, 2013.

50. A. Mason, G. Hamer, ***Survival and activity of Klebsiella pneumoniae at super-optimal temperatures***, **Bioprocess and Biosystems Engineering**, 2:121-127, 1987.

51. https://www.jstor.org/stable/30144997?seq=1#page_scan_tab_content, accessed at 18th July 2017.

52. I. Pinchuk, E. Beswick, V.Reyes, ***Staphylococcal Enterotoxins***, **Toxins (Basel)**, 2:2177–2197, 2010.

53. I. Brook, ***Anaerobic Infections: Diagnosis and Management***, **Informa healthcare Inc.**, USA, 2008

54. J. Kong, L.Chia , N. Goh ,T. Chia , R. Brouillard, ***Analysis and biological activities of Anthocyanins***, **Phytochemistry**, 64:923-933, 2003.

55. O. Zarkotou, S. Pournaras, P. Tselioti, V. Dragoumanos, V. Pitiriga, K. Ranellou, A. Prekates, K. Themeli-Digalaki, A. Tsakris, ***Predictors of mortality in patients with bloodstream infections caused by KPC-producing Klebsiella pneumoniae and impact of appropriate antimicrobial treatment***, **Clinical Microbiology and Infection**, 17:1798–1803, 2011.

56. L. Pagano, M. Caira, E. Trecarichi, T. Spanu, R. Blasi, S. Sica, M. Sanguinetti, M. Tumbarello, ***Carbapenemaseproducing Klebsiella pneumoniae and Hematologic Malignancies***, **Emerging Infectious Diseases**, 20, 2014.

57. N. Hearn, ***Chlorine in Drinking Water the Good, the Bad & the Ugly News***, Available at:

http://www.waterbenefitshealth.com/chlorine-in-drinking-water.html, accessed 27th Dec 2017.

58. ***Six technologies that produce clean, safe drinking water***, Available at: https://www.engadget.com/2016/09/17/six-technologies-that-produce-clean-safe-drinking-water, accessed 1st Jan 2018.
59. ***ZINC Oxide***, **National Center for Biotechnology Information**, U.S. National Library of Medicine. Available at: https://pubchem.ncbi.nlm.nih.gov/compound/zinc_oxide#section=Solubility, accessed 19th Jan 2018.
60. M. Gross, S. Cramton, F. Götz, A. Peschel, ***Key Role of Teichoic Acid Net Charge in Staphylococcus Aureus Colonization of Artificial Surfaces***, **Infection and immunity**, 69: 3423–342, 2001.
61. E. Frirdich, C. Bouwman, E. Vinogradov, C. Whitfield, ***The Role of Galacturonic Acid in Outer Membrane Stability in Klebsiella pneumonia***, **The American Society for Biochemistry and Molecular Biology**, 280: 27604-27612, 2005.
62. N. Daneshvar, S. Aber, M. S. Seyed Dorraji, A. R. Khataee, and M. H. Rasoulifard***, "Preparation and Investigation of Photocatalytic Properties of ZnO Nanocrystals: Effect of Operational Parameters and Kinetic Study"***, **International Journal of Chemical and Biomolecular Engineering**, 1:24-29, 2008.
63. A. Vidyasagar, ***What Are Bacteria? Live Science Contributor***, Available at: https://www.livescience.com/51641-bacteria.html, accessed 22th Jan 2018.

64. S. Wahyuningsih, L. Wulandari, M. Wartono, H Munawaroh, A. Ramelan, ***The Effect of pH and Color Stability of Anthocyanin on Food Colorant, IOP Conference Series***, **Materials Science and Engineering**, 299, 2018.
65. ***XRD Crystallite Size Calculator (Scherrer Equation)***, **InstaNANO**, Available at: https://instanano.com/characterization/theoretical/xrd-size-calculation,accessed 20 Mar. 2018
66. C. Lok, C. Ho, R. Chen, Q. He, W. Yu, H. Sun, H. Tam, J. Chiu, C. Che, ***Proteomic analysis of the mode of antibacterial action of silver nanoparticles***, **J. Proteome Res**, 5:916–924, 2006.
67. H. Meruvu, M. Vangalapati, S. Chippada, S. Bammidi, ***Synthesis andcharacterization of Zinc Oxide nanoparticles and its antimicrobial activity against Bacillus subtilis and Escherichia coli***, **Rasayan journal of chemistry**, 4:217–222, 2011.
68. N. Amro, L. Kotra, K. Wadu-Mesthrige, A. Bulychev, S. Mobashery, G. Liu, ***High-resolution atomic force microscopy studies of the Escherichia coli outer membrane: structural basis for permeability***, **Langmuir**, 16:2789–2796, 2000.
69. M. Premanathan, K. Karthikeyan, K. Jeyasubramanian, G. Manivannan, ***Selective toxicity of ZnO nanoparticles toward G-positive bacteria and cancer cells by apoptosis through lipid peroxidation***, **Nanomed Nanotechnol Biology and Medicine**, **7**:184–192,2011.
70. W. Song, J. Zhang, J. Guo, J. Zhang, F. Ding, L. Li, Z. Sun, ***Role of the dissolved zinc ion and reactive oxygen species in cytotoxicity of ZnO nanoparticles***, **Journal of Toxicology Letters,** 199:389–397, 2010.

71. M. Heinlaan, A. Ivask, I. Blinova, H.-C. Dubourguier, A. Kahru, ***Toxicity ofnanosized and bulk ZnO, CuO and TiO_2 to bacteria Vibriofischeri and crustaceans Daphniamagna and Thamnocephalus platyurus***, **Chemosphere**, 71:1308–1316, 2008.

72. B. Sevinç, L. Hanley, ***Antibacterial activity of dental composites containing zinc oxide nanoparticles***, **Journal of Biomedical Materials Research Part B**, 94:22–31, 2010

73. R. Brayner, R. Ferrari-Iliou, N. Brivois, S. Djediat, M.F. Benedetti, F. Fiévet, ***Toxicological impact studies based on Escherichia coli bacteria in ultrafine ZnO nanoparticles colloidal medium***, **Nano Letters (ACS Publications) - American Chemical Society**, 6:866–870, 2006.

74. L. Zhang, Y. Jiang, Y. Ding, M. Povey, D. York, ***Investigation into the antibacterial behaviour of suspensions of ZnO nanoparticles (ZnO nanofluids)***, **Journal of Nanoparticle Research**, 9:479–489, 2007.

75. A. Tsuji, Y. Kaneko, K. Takahashi, M. Ogawa, S. Goto, ***The Effects of Temperature and pH on the Growth of Eight Enteric and Nine Glucose Non-Fermenting Species of G-Negative Rods***, **Microbiology Immunology**, 26:15-24, 1982.

76. M. Paczosa, J. Mecsas, **Klebsiella pneumoniae: Going on the Offense with a Strong Defense**, **Microbiology and Molecular Biology Reviews**, 80:629–661, 2016.

77. M. Schweizer, L.Herwaldt, ***G positive bacteria - Staphylococcus aureus***, Available at:

https://www.infectiousdiseaseadvisor.com/hospital-infection-control/G-positive-bacteria--staphylococcus-aureus/article/598956, accessed 30 Mar. 2018.

78. A. Sirelkhatim, S. Mahmud, A. Seeni, N. Haida, M. Kaus, L. Ann, S. Khadijah, M. Bakhori, H. Hasan, D. Mohamad, ***Review on Zinc Oxide Nanoparticles: Antibacterial Activity and Toxicity Mechanism***, **Springer Berlin Heidelberg**,**7**:219–242,2015.
79. K. Hirota, M. Sugimoto, M. Kato, K. Tsukagoshi, T. Tanigawa, H. Sugimoto, ***Preparation of Zinc Oxide ceramics with a sustainable antibacterial activity under darkconditions***, **Ceramics International**, **36**:497–506, 2010.
80. I. Kirkinezos, C. Moraes, ***Reactive oxygenspecies and mitochondrial diseases***. **Journal of Seminars in Cell and Developmental Biology**,**12**:449–457, 2001.
81. ***The Beer -Lambert Law***, Available at: https://www.chemguide.co.uk/analysis/uvvisible/beerlambert.html, accessed 31 Mar. 2018.
82. D. Truhlar, ***Essay Valence Bond Theory for Chemical Dynamics***, https://pdfs.semanticscholar.org/197b/77605940c84e18e47a6ed39a020d424b6ffe.pdf,accessed in 11th June 2017.
83. H. Chang, Y.Lo, ***Pomegranate leaves and mulberry fruit as natural sensitizers for dye-sensitized solar cells***, **Solar Energy**, 84: 833-1837, 2010.

84. E. Meulenkamp, ***Synthesis and Growth of ZnO Nanoparticles***, **American Chemical Society**, 102:5566

جامعة النجاح الوطنية
كلية الدراسات العليا

التحطيم الضوئي لبكتيريا موجبة وسالبة الغرام في الماء مع مكوناتها العضوية باستخدام حبيبات أكسيد الزنك النانوية والاصباغ

إعداد
سوسن فتحي عبد السلام جابر

إشراف
أ. د. حكمت هلال
د. مجدي دويكات

قدمت هذه الأطروحة استكمالا لمتطلبات الحصول على درجة الماجستير في الكيمياء بكلية الدراسات العليا في جامعة النجاح الوطنية في نابلس، فلسطين.
2018

التحطيم الضوئي لبكتيريا موجبة وسالبة الغرام في الماء مع مكوناتها العضوية باستخدام حبيبات أكسيد الزنك النانوية والاصباغ.

إعداد

سوسن فتحي عبد السلام جابر

إشراف

أ. د. حكمت هلال

د. مجدي دويكات

الملخص

تنقية المياه وتطهيرها من الملوثات المختلفة أصبح ضرورة لحياة كريمة للفرد، حيث يتم إتباع استراتيجيات مختلفة في دول عدة من اجل تنقية المياه، أفضل الطرق هي الطريقة الآمنة على صحة الإنسان وذات الكفاءة العالية والتكلفة المنخفضة. إن التحطيم الضوئي للبكتيريا يعتبر من أكثر الطرق كفاءة وجذبا لاهتمام الباحثين في هذا المجال، حيث يتم تحفيز أشباه الموصلات باستخدام الضوء والذي يقوم بدوره بالتحطيم الضوئي للملوثات البيولوجية والكيميائية المتواجدة في الماء حيث أصبحت حبيبات أكسيد الزنك (ZnO) النانوية تستخدم على نطاق واسع لكثير من الملوثات العضوية للماء. إن حبيبات أكسيد الزنك (ZnO)التي تمتلك فجوة طاقة (Band gap) واسعة (3.2eV) تحتاج إلى طول موجة يتواجد في منطقة الأشعة فوق البنفسجية حيث يقتصر النشاط التحفيزي على أطوال موجات أقصر تقع فهذه المنطقة. وبما أن 4٪ فقط من الطيف الشمسي تقع في منطقة الأشعة فوق البنفسجية، فإن استخدام الأصباغ الطبيعية، مثل صبغة الأنثوسيانين الطبيعية (Anthocyanin) المستخلصة من أزهار نبات الكركدية والتي تساعد أكسيد الزنك (ZnO) من الاستفادة من ضوء الشمس المرئي أصبح ضروريا لزيادة كفاءة الحفاز لقتل البكتيريا الملوثة للمياه.

في هذا العمل تم تعقيم المياه عن طريق التحطيم الكامل لنوعي البكتيريا إيجابية الغرام (*Staphylococcus aureus*) والسالبة الجرام (*Klebsiella pneumoniae*) جنبا إلى جنب مع مكوناتها العضوية وذلك باستخدام جزيئات أكسيد الزنك (ZnO) النانوية حيث بعد 60 دقيقة تم التخلص من نوعي البكتيريا بشكل كامل، بعد 3 ساعات تم تحطيم 98.7% من المكونات العضوية

الخاصة بالبكتيريا موجبة الغرام و45.2% من المكونات العضوية الخاصة بالبكتيريا سالبة الغرام بفضل أشعة ضوئية من فئة الأشعة الشمسية. وقد تم التوصل إلى هذه النتائج في نوعي البكتيريا المستخدمين لأول مرة. ولقد تمت دراسة أثر بعض العوامل على فعالية الحفاز وسير تفاعل التحطيم الضوئية مثلما الإشعاع، درجة الحرارة، درجة الحموضة، تركيز كل من الحفاز والملوث وأخيرا أثر حركة المحلول على سير التفاعل الضوئي. هذا وقد تبين إن الحفاز ZnO يمكن فصله وإعادة استخدامه، دون خسارة في كفاءته النسبية، لمرتين متتاليتين.